

Controlled-Source Electromagnetic Approaches for Hydrocarbon Exploration and Monitoring on Land

Rita Streich¹

Received: 22 October 2014 / Accepted: 14 August 2015 / Published online: 3 September 2015
© Springer Science+Business Media Dordrecht 2015

Abstract Electromagnetic methods that utilize controlled sources have been applied for natural resource exploration for more than a century. Nevertheless, concomitant with the recent adoption of marine controlled-source electromagnetics (CSEM) by the hydrocarbon industry, the overall usefulness of CSEM methods on land has been questioned within the industry. Truly, there are few published examples of land CSEM surveys carried out completely analogously to the current marine CSEM standard approach of towing a bipole source across an array of stationary receivers, continuously transmitting a low-frequency signal and interpreting the data in the frequency domain. Rather, different sensitivity properties of different exploration targets in diverse geological settings, gradual advances in theoretical understanding, acquisition and computer technology, and different schools in different parts of the world have resulted in a sometimes confusing multitude of land-based controlled-source EM surveying approaches. Here, I aim to review previous and present-day approaches, and provide reasoning for their diversity. I focus on surface-based techniques while excluding airborne EM and well logging and on applications for hydrocarbon exploration. Attempts at the very demanding task of using onshore controlled-source EM for reservoir monitoring are shown, and the possible future potential of EM monitoring is discussed.

Keywords Controlled-source electromagnetic · Hydrocarbon exploration · Onshore · Monitoring

1 Introduction

Electromagnetic (EM) methods, attempting to detect contrasts in electrical resistivity between target resources and their surroundings, have been developed and utilized for exploring buried resources for more than a century. Since the first well-documented

✉ Rita Streich
rita.streich@shell.com

¹ Shell Global Solutions International BV, Kesslerpark 1, 2288 GS Rijswijk, The Netherlands

electric sounding carried out by the Schlumberger brothers (Schlumberger 1920), our understanding of electromagnetic field behavior has evolved tremendously and been captured in various textbooks (Wait 1962; Keller and Frischknecht 1966; Kaufman and Keller 1983; Nabighian 1988; Zhdanov and Keller 1994). These continue to be standard references for many EM researchers today. There may be a notion that fundamental EM theory and concepts are now thoroughly understood, yet to this date new books (Zhdanov 2009; Kaufman et al. 2014) and articles addressing very fundamental questions (e.g., Gómez-Treviño and Esparza 2014) continue to appear. Likewise, a multitude of practical EM surveying approaches and hardware has been developed (e.g., Nabighian 1991; Strack 1992). The status has been reviewed, and predictions on future developments have been made at various points throughout the history of controlled-source EM (e.g., Rust 1938; Nekut and Spies 1989; Sheard et al. 2005; Strack 2014).

Earlier reviews covered land EM (as opposed to marine EM) without explicitly mentioning that this was their focus (Ward 1980). Historically, EM had been in use on land long before its marine application started to be investigated. Nevertheless, the recent rediscovery of marine controlled-source EM for hydrocarbon reservoir imaging (Eidesmo et al. 2002; Ellingsrud et al. 2002; Ziolkowski et al. 2002; Srmka et al. 2006; MacGregor et al. 2006) certainly sparked new interest in EM methodology in general. From a marine CSEM perspective, questions have been raised within the hydrocarbon industry on the overall usefulness of CSEM on land. It therefore seems timely to review the existing technology for onshore controlled-source EM exploration. The underlying physical principles are, of course, the same in onshore and offshore environments. Nevertheless, the presence or absence of water strongly influences the observable EM field. Therefore, techniques of surveying and data interpretation tend to differ significantly, depending upon the target we wish to illuminate.

From the perspective of the present-day marine CSEM business, the topic of “land controlled-source EM exploration” may be interpreted as narrowly as to comprise only the surveying approach analogous to today’s standard marine acquisition. This would mean surveying with grounded bipole sources, emitting low-frequency square waves or variants thereof and interpreting the data in the frequency domain. Yet in many cases, this is not optimum for land CSEM surveying. Neither would such a narrow interpretation do justice to the rich history, wide variety, versatility, and full imaging power of land controlled-source EM technology. Conversely, “land controlled-source EM exploration” can also be interpreted as widely as to cover a major part of the EM work done throughout history, only excluding natural-source magnetotellurics (MT) and the historically relatively small, yet currently important field of marine CSEM applications. “Exploration” in a wider sense can include the search for any buried resources, such as minerals, hydrocarbons, geothermal energy, or groundwater.

It is impossible to cover land EM exploration in the widest sense within a single paper. Therefore, in this review, I will take an intermediate approach. I will consider a range of surveying techniques developed throughout EM history, and attempt to illuminate reasons for the existence of the sometimes confusing variety of approaches and corresponding acronyms. I will not consider airborne EM (for a recent review, see, e.g., Siemon et al. 2009), well logging (e.g., Kaufman and Dashevsky 2003; Davydycheva 2010), or cross-well techniques. Instead, I will focus on surface-based surveying and include attempts at borehole-to-surface measurements. I will focus on hydrocarbon exploration targets, mostly leaving out mining applications. These doubtlessly constitute a prime field of application of EM techniques, as described, e.g., in a recent review by Smith (2014). I will only marginally touch upon other targets such as geothermal reservoirs (Muñoz 2014),

geological storage sites (e.g., Gasperikova and Hoversten 2006; Zhdanov et al. 2013), and near-surface applications (Everett 2012).

2 Milestones of Land EM History

First applications of electromagnetic techniques date back at least as far as to the measurements of self potentials in a copper mine by Fox (1830). Long before the unit of ampere was defined, Fox described current strength in terms of rotation of his galvanometer. Decades before the periodic table of elements was put down, he correctly linked different current strengths to the presence of different metals.

First attempts at surveying with an active source were probably made early in the twentieth century. Daft and Williams (1906) used the relatively new invention of the telephone for localizing mineral deposits by listening to the Earth's response to transient impulses. The same "telephonic method" was also applied in Sweden by Petersson (1907) with mixed success, partly complicated by the presence of metallic infrastructure obscuring the signals. However, transient surveying was not more widely adopted before the well-trained operator's ear was replaced by more quantitative recording equipment. The first largely successful surveys with an active source are probably the direct current (DC) measurements carried out by the Schlumberger brothers (Schlumberger 1920). Conrad Schlumberger develops fundamental concepts of DC resistivity surveying, electrical potentials and even resistivity anisotropy. Experiments with alternating current (AC) using telephones led him to the important observation that inductive phenomena strongly influenced those measurements. He abandons this approach, though, and discredits his own and other contemporaneous attempts at alternating current measurements as being impractical and too complicated to deliver interpretable results. He also describes induced-polarization phenomena observed upon interrupting current circuits, yet dismisses their measurement in favor of "spontaneous polarization," i.e., self-potentials (Schlumberger 1920).

Ward (1980) summarizes further foundations of EM methods laid in the 1920s and 1930s primarily in the domain of the mining industry. Inspired by the success of EM for mineral exploration, investigations on using EM for oil exploration started soon (e.g., Hedstrom 1930), and even the integration of EM with other geophysical and well data was considered (Gish 1932). Problems which continue to hamper EM surveys to date were recognized, such as the general possibility of obtaining ambiguous results (Jenny 1930), responses of target features being obscured by stronger responses of nearby or overlying units, and difficulty in distinguishing between a layer of very high resistivity and a layer whose resistivity is only moderately elevated from the background (Sundberg 1930). Measurement configurations of optimum sensitivity to resistors had yet to be found, although galvanic sources were already in use (Jenny 1930).

Hydrocarbon accumulations tended to be located at greater depths than typical targets encountered in mineral exploration (Nekut and Spies 1989). As resources are becoming depleted and deeper targets embedded in increasingly complex geological structure are being accessed, limits of depth penetration continue to present a significant challenge for hydrocarbon exploration. In an early overview of EM for hydrocarbon exploration, Peters and Bardeen (1932) rebut "extravagant claims" that the depth of investigation achievable by EM methods be up to 1500 m. They estimate it to be no more than about 450 m with measuring apparatus available at the time. Consequently, they describe an approach for structural imaging of oil reservoirs by tracing shallow conductive marker beds, assuming

that these are approximately parallel to deeper oil-bearing layers where geological conditions are relatively simple (also detailed by Sundberg 1930). Not surprisingly, this approach produced mixed outcomes. One of their main conclusions is still valid today: exaggerations regarding the capabilities of EM have repeatedly brought the entire method into disrepute.

About the same time, the feasibility, or otherwise, of direct hydrocarbon detection by EM methods already was a subject of controversial debate (Gella 1930; Heiland 1932). Karcher and McDermot (1935) recognize that in order to penetrate to depths at which oil reservoirs are commonly encountered, frequencies have to be lowered to one Hz and less, and describe a surveying approach that includes periodic switch-off of the source. Instruments and surveying techniques for transient measurements are also described by Blau (1933) and in a subsequent series of patents, which additionally claim that reflections from subsurface layers would directly be visible in transients (Blau 1933; Melton 1937; Statham 1939; Blau and Statham 1939, 1940). This was later disproven by Yost (1952). Further to this work, Statham (1936) describes the concept of current diffusion later termed “smoke rings” (Nabighian 1979). From field measurements, Statham (1936) finds anomalies corresponding to known lateral geological boundaries, without explicitly determining resistivity values, and without attempting to identify individual layers from the shape of the transients.

Subsequent to the publication of the seminal book by Stratton (1941), major theoretical advances were made. Analytical solutions were derived for different source types (e.g., Wait 1951a, 1954), 1D layered media (Wait 1962), and other basic geometries of practical importance (Wait 1951b, 1952). Real-world problems such as anisotropy were investigated (Maillet 1947). Foundations for later numerical solutions were laid (Hestenes and Stiefel 1952). Surveying techniques were further developed (Enslin 1955), and instruments that allowed faster and more accurate recordings under variable coupling conditions were constructed (Guelke 1945; Bellairs 1955).

For several decades to follow, developments went on largely independently on both sides of the Iron Curtain (Spies 1983). To this date, approaches followed in the East and West may not be fully appreciated on the respective other side (see, e.g., recent discussion by Nabighian 2012; Zhdanov 2012), with mutual understanding sometimes being hampered by differences in nomenclature and language barriers. Significant development was carried out in Russia on EM theory (e.g., Vanyan et al. 1967), modeling (e.g., Druskin and Knizhnerman 1988), inversion, and the regularization that now is named after its developer (Tikhonov and Arsenin 1977). The utility of time-domain approaches was universally recognized (Wait 1951a; Vanyan et al. 1967; McCracken et al. 1980; Wait 1982; Spies 1983). Experiments with very large and high-power sources were carried out (e.g., Keller et al. 1984; Velikhov et al. 1987; Zhdanov 2010) under vigilant attention of and supported by the military (Freeman 1987).

EM methodology continues to evolve, in line with our improving theoretical understanding, and technology advancements permit new generations of transmission and recording hardware to be designed. Steadily growing computing capabilities allow us to use more sophisticated processing and imaging tools. Accordingly, data interpretation techniques have evolved from comparison of sounding curves to precalculated type curves for 1D models containing few layers over 1D inversion (e.g., Glenn et al. 1973; Jupp and Vozoff 1975; Constable et al. 1987) to 2D (Oristaglio and Worthington 1980; Wang et al. 1994), 2.5D (e.g., Torres-Verdín and Habashy 1994; Unsworth and Oldenburg 1995), and 3D (e.g., Newman and Alumbaugh 1997) inversion and interpretation.

3 The Challenge of Detecting Resistors

For many sedimentary formations, bulk resistivity is primarily determined by pore fluid content, and porosity, pore shape, and connectivity. Hydrocarbons are generally more resistive than saline pore water. Therefore, when exploring hydrocarbon reservoirs, we are most commonly faced with the task of identifying electrically resistive features in a more conductive environment. The opposite situation of conductive targets within resistive embedding is only occasionally encountered in hydrocarbon exploration. Examples include the imaging of highly conductive brine underneath an oil field (Duckworth and O'Neill 1989), the search for lenses of unfrozen water usable for oil production within permafrost regions (Antonov et al. 2014), or attempts of imaging moderately conductive sediments underneath resistive basalt cover (Wilt et al. 1989; Morrison et al. 1996).

Earlier systematic studies on detecting resistive layers in conductive surroundings include Eadie (1980) and Passalacqua (1983). The simple example shown in Fig. 1 demonstrates that this is significantly more challenging than the opposite situation of searching for conductors within resistive embedding. EM fields are displayed for simple models of a resistive layer embedded in a more conductive half-space, a conductive layer embedded in a resistive half-space (Fig. 1a), and the respective half-space background

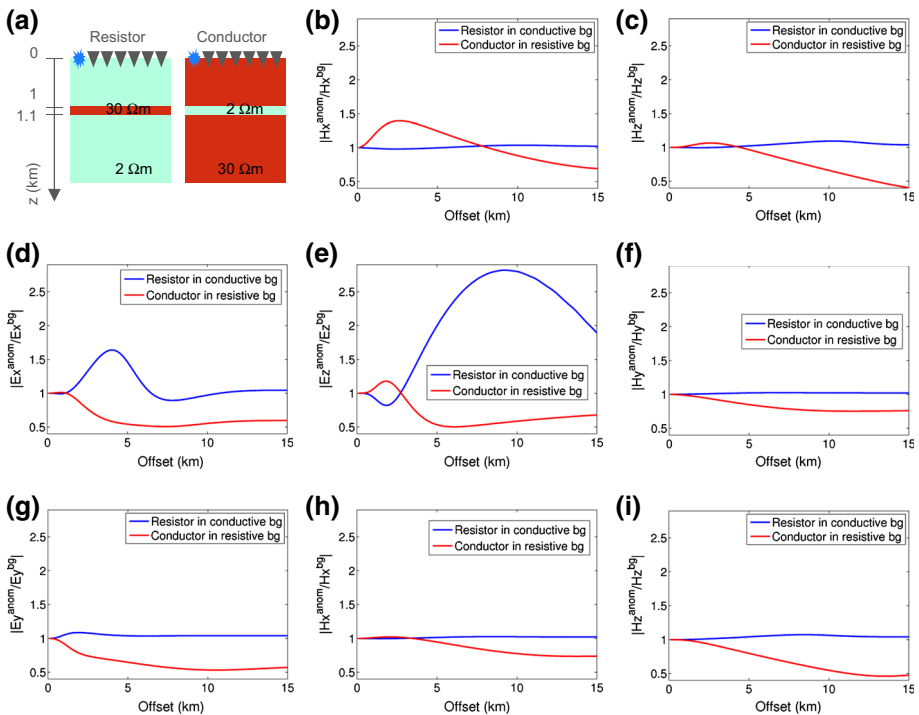


Fig. 1 **a** Canonical models of a resistor embedded in conductive background (bg) and a conductor embedded in resistive background. **b–i** Ratios of fields for the models with the anomalous (anom) layers to the fields for the respective background models at frequency 0.2 Hz for the resistor and 1 Hz for the conductor. **b** Vertical magnetic dipole (VMD) source and field component H_x, **c** VMD and H_z, **d** x-directed horizontal electric dipole (HED) and inline E_x, **e** x-directed HED and E_z, **f** x-directed HED and H_y, **g** y-directed HED and E_y (i.e., broadside configuration), **h** y-directed HED and H_x, **i** y-directed HED and H_z

models. Horizontal electric dipole (HED), vertical electric dipole (VED), horizontal magnetic dipole (HMD), and vertical magnetic dipole (VMD) sources are considered. A line of receivers of vector electric and magnetic fields is placed along the x axis. Considering the different skin depths, frequencies of 0.2 Hz and 1 Hz are used for the conductive and resistive half-spaces, respectively.

Figure 1b–i shows those combinations of source types and EM field components for which amplitudes between fields for the layered and background models differ by more than 10 % (equivalent reciprocal configurations are not shown). For the conductor in a resistive half-space, this crude detectability threshold is exceeded by all of the source–receiver configurations shown. In principle, all of these geometries and their reciprocal configurations (e.g., exchanging the broadside HED and H_z in Fig. 1i by a VMD and E_y) can thus be used for imaging the conductive layer. In contrast, only the inline HED– E_x and inline HED– E_z configurations (Fig. 1d, e) show a significant anomaly for the resistor in a conductive half-space. For the HED– E_z geometry, field amplitudes are small, falling below an optimistic noise floor of 10^{-16} V/(Am²) at offsets of about 5 km for the resistor model and 9 km for the conductor model. The choice of geometries suitable for imaging conductors is thus rather limited. Of course, to avoid “anomaly hunting” and obtain a full 3D image of subsurface resistivity structure, 3D rather than line geometries should be considered. Yet this does not eliminate the principal difficulty of imaging resistive features. The poor visibility of resistors to most source–receiver geometries is related to currents preferably flowing within more conductive bodies. The relatively good visibility of resistors to the inline HED– E_x and E_z configurations is associated with the guided-wave mode developing and propagating within the resistive layer (e.g., Weidelt 2007a; Chave 2009).

3.1 Approximate Plane-Wave Sources

In addition to the source–receiver configurations discussed above, approximate plane-wave source fields have been generated using controlled sources. This approach, referred to as controlled-source audio-magnetotellurics (CSAMT), was originally introduced as a method that worked analogously to natural-source magnetotellurics, but provided a more reliable source than MT (Goldstein and Strangway 1975; Sandberg and Hohmann 1982; Zonge and Hughes 1991; Tang and He 2000). At first order, the excited source field arrives at the receiver as plane waves, diffusing vertically into the Earth (Goldstein and Strangway 1975; Wannamaker 1997). Therefore, CSAMT is thought to primarily image the subsurface near the receiver.

Similar to natural-source magnetotellurics, CSAMT is particularly well suited and thus primarily being applied for imaging conductors within a more resistive background. Accordingly, CSAMT has only found limited application for hydrocarbon targets. Examples include the structural imaging of atypical oil fields where the oil is embedded in volcanic rocks and thus forms a conductive zone (Hughes and Carlson 1987) or the imaging of conductive coal beds underneath a highly resistive overburden of volcanic rocks (An and Di 2010).

3.2 “Air Waves”

The parts of the EM field propagating through the air, directly and after interaction with the subsurface, have been identified as major obstructions reducing the relative influence of

subsurface features on EM field recordings. Comparison of EM responses for land and marine settings demonstrates this issue (Fig. 2). In the marine case, the source signal excited near the seafloor first propagates up through the water, thereby becoming significantly attenuated. A “refracted wave” mode is then formed and, finally, the signal propagates back down to the receivers, thereby undergoing further attenuation (e.g., Constable and Weiss 2006). As a consequence, signal that has propagated through the air becomes dominant only at far offsets larger than 10 km in the example shown, as indicated by the change in slope of the amplitude-versus-offset curve. In contrast, the “air wave” starts dominating at much shorter offsets on land (about 6 km in Fig. 2). The resistive layer generates a large amplitude anomaly for the marine case at offsets near 10 km, and a still significant, but smaller anomaly at about 4–5 km offset for the land case (Fig. 2c). In addition, the resistive layer influences signal phase much more strongly in the marine than in the land case (Fig. 2b). On land, phase approaches zero at large offsets, corresponding to the dominant portion of the signal propagating virtually instantaneously at the speed of light in air.

Various remedies for reducing the dominance of the “air wave” have been proposed. For example, an approach by Weidelt (2007a, b) is based on the insight that for 1D layered models, the radial (inline) field E_r , and tangential (broadside) field E_ϕ at identical source–receiver distances differ by a factor of two, and the tangential field is nearly free of air-coupled models. Therefore, approximate airwave removal is achieved by taking

$$E_r(r, \phi = 0^\circ)^{no\ air} \approx E_r(r, \phi = 0^\circ)^{with\ air} - \frac{1}{2}E_\phi(r, \phi = 90^\circ)^{with\ air}, \quad (1)$$

where angles $\phi = 0^\circ$ and 90° denote the inline and broadside configurations, respectively. Figure 3 illustrates that this relation indeed holds approximately, yet not exactly. This is similarly true for other proposed airwave removal techniques (Løseth et al. 2010; Chen and Alumbaugh 2011; Wirianto et al. 2011). Therefore, instead of possibly introducing error from approximate airwave removal based on assumptions that do not hold exactly, including the airwave in forward models has become a commonly adopted solution (Plessix et al. 2007; Commer and Newman 2009; Grayver et al. 2014).

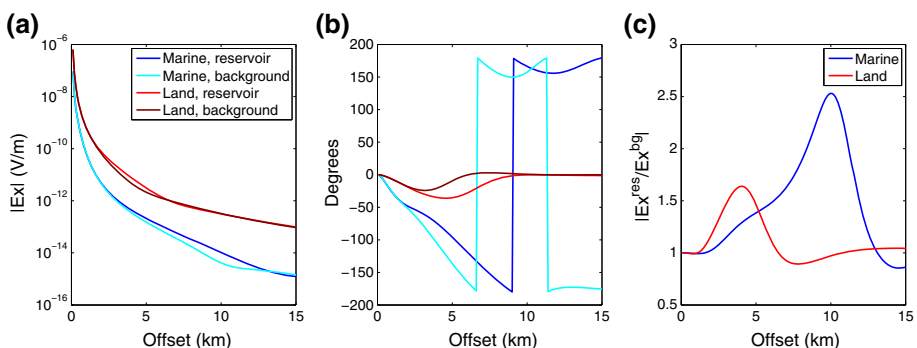


Fig. 2 **a** Amplitude and **b** phase of the inline electric field for the resistive layer model shown in Fig. 1a, the background half-space model, and analogous marine models with a 1-km-thick water layer ($\rho = 0.33 \Omega\text{m}$) on top, frequency 0.2 Hz. **c** Amplitude ratios between the resistive-layer and background models

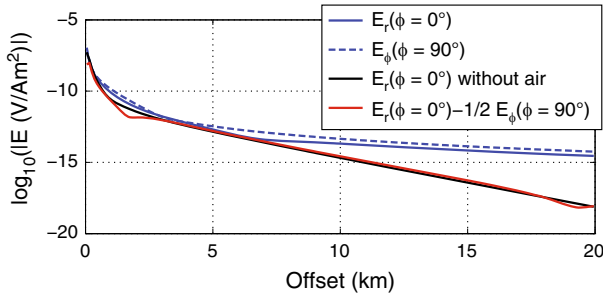


Fig. 3 Approximate airwave removal according to Weidelt (2007a). The blue solid and dashed lines show the radial (inline) and tangential (broadside) fields for a 1D model containing an air half-space. The black line denotes the exact field if the air is removed from the model. The red line denotes the field in which the airwave is removed approximately using Eq. 1

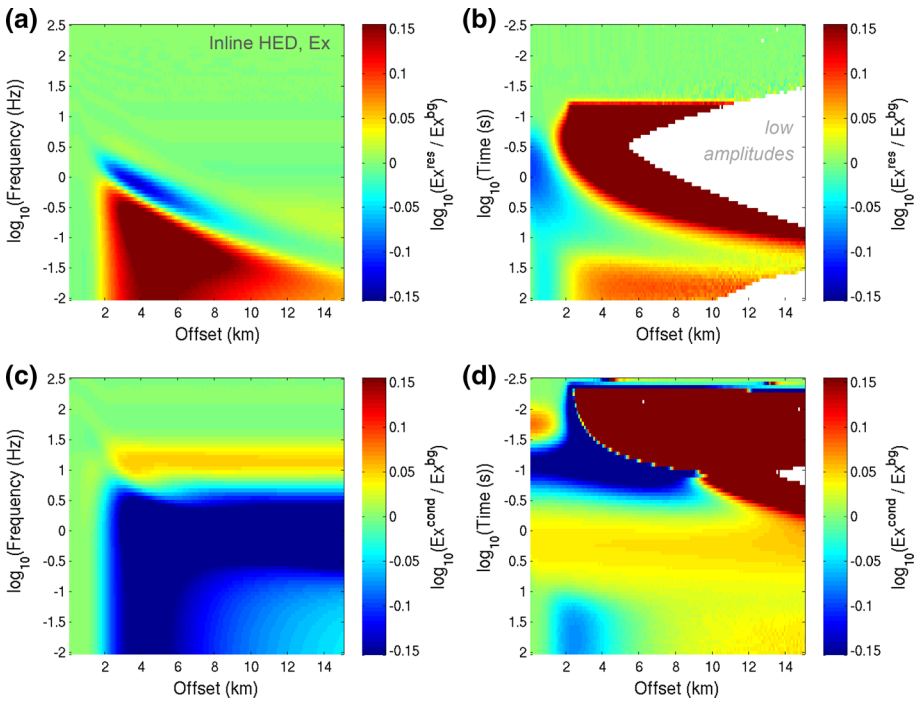


Fig. 4 Amplitude ratio between data for **a, b** the resistive-layer model from Fig. 1a and its background half-space and **c, d** the conductive-layer model and corresponding background half-space, for an inline HED–Ex configuration. In **(a)** and **(c)**, frequency-domain data are displayed. **b, d** Time-domain data (impulse responses) for a time range equivalent to the frequency range displayed in **(a)** and **(c)**. Regions where amplitudes fall below 10^{-15} V/m have been blanked

3.3 Frequency or Time Domain?

Measurements of transients and data interpretation in the time domain offer yet another potential way of reducing the dominance of airwave signal. Time- and frequency-domain

data are uniquely related by the mathematical operation of the Fourier transform and are thus equivalent in principle. As with other transforms that aim to separate signal and noise or different portions of the signal, such as the wavelet or Radon transforms, representations of EM data in either domain may highlight different parts of the information contained in the data.

For land-based surveys, recording of transients during transmitter-off time, or equivalent recovery of transients from recorded time series, has repeatedly been advocated (e.g., McCracken et al. 1980; Frischknecht and Raab 1984; Strack 1992; Ziolkowski et al. 2007; Zhdanov 2010). The underlying idea is that the part of the EM field propagating directly through the air from the source to the receiver at the speed of light in air is separated in time from subsurface response that propagates more slowly and thus arrives at later times. Therefore, analyzing the EM field decay after the direct field has passed the receiver should permit looking deep at short source–receiver distances.

This concept is illustrated in Figs. 4 and 5 for the models from Fig. 1a and the inline HED–Ex and broadside HED–Ey geometries, respectively. The direct field, which carries no subsurface information, is a sharp pulse in the time domain and, correspondingly, very broadband signal in the frequency domain. At short offsets, this signal is much stronger than signal returned from the subsurface and thus masks any subsurface response in the frequency domain (Figs. 4a, c, 5a, c).

Remarkably, when using the broadside HED–Ey geometry, the resistive layer studied here generates a significantly stronger anomaly in the time domain than in the frequency domain (Fig. 5a, b). It may thus become detectable when interpreting the data in the time

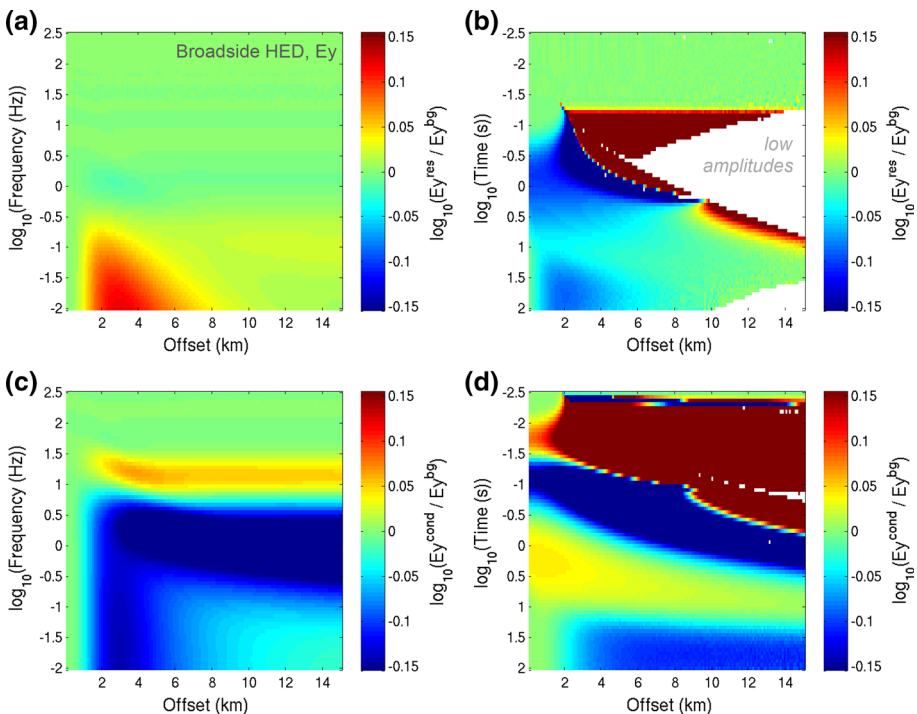


Fig. 5 As for Fig. 4, but for a broadside HED–Ey geometry

domain. In contrast, it would likely be invisible in the frequency domain (Figs. 1g, 5a) or only be visible at ultra low frequencies near 1/100 Hz that would be impractical to record with sufficient stacking for obtaining adequate signal-to-noise ratios. The time-domain imaging capability of the broadside HED–Ey geometry is exploited by the long-offset transient EM (LOTEM) technique (Strack et al. 1989a; Strack 1992).

Further practical complications may render frequency- and time-domain measurements non-equivalent (Kaufman 1989). One such complication is the availability of suitable recording apparatus. Transient EM fields were measured quite early in the history of EM development (e.g., Statham 1936). However, accurate transient measurements require generating sufficiently sharp, precisely repeatable step function signals and recording them accurately over wide dynamic ranges, from very early to late times. This requires more advanced electronic components than generating and recording the mono-frequency sine wave signals used by early frequency-domain systems (McCracken et al. 1986a). That may be a reason why time-domain recording evolved somewhat later than frequency-domain recording and became widely used only in the 1970s and 1980s (e.g., McCracken et al. 1980; Nabighian and Macnae 1991). Most modern EM systems, though, use advanced hardware and step function-type signals regardless of the domain of data interpretation.

As hardware evolved, various source time functions were tested, such as triangular waveforms that permitted directly measuring step responses of the subsurface (West et al. 1984), and frequency sweeps similar to those used in vibroseis (Won 1980). Transients have also been derived from pseudo-random binary sequences (Duncan et al. 1980; Gómez-Trevino and Edwards 1983; Helwig 1998; Ziolkowski et al. 2007). For earlier systems designed for recording transients, it was commonly assumed that source switching occurred instantaneously and source currents were known precisely. Accordingly, the system characteristic of the transmitter was not routinely corrected for, although principles and advantages of system response correction were known (Strack 1992). More recent data confirm that deconvolving the transmitter response improves the accuracy of transients (Wright et al. 2005). In combination with a multichannel receiver layout, the approach of deriving impulse responses by deconvolving the recorded source signal from every individual recorded transient was commercialized (McBarnet and Ziolkowski 2005) and became known under the acronym MTEM (multichannel transient electromagnetics; Wilson 1997).

Conversely, frequency-domain recording approaches up until the 1980s may have put frequency-domain data at a somewhat unnecessary disadvantage. Attempts were made then to remove the primary field during the measurement process using approximate compensation techniques, such that, in principle, only the secondary field should have been recorded. This, however, is an error-prone procedure that introduced inaccuracy into frequency-domain recordings. This weakness of frequency-domain recordings certainly contributed to the widely reported preference for time- over frequency-domain data (McCracken et al. 1986a), although frequency-domain systems existed that transmitted mono-frequency signal and still permitted full-field recording (Hohmann et al. 1978).

Today's high-fidelity recording systems are capable of measuring the very widely varying amplitudes of total rather than secondary EM fields. Likewise, high-frequency A/D converters are available for recording transients accurately. "Time-domain" and "frequency-domain" acquisitions can employ identical hardware and typically differ only by the use of source time functions that do or do not include transmitter-off times. Accordingly, decisions on the domain to use can be made at the interpretation stage. The choice of frequency- or time-domain interpretation should primarily be guided by the sensitivity properties of the exploration target at hand.

3.4 Attempts to Enhance Sensitivity

Very commonly, in EM exploration we operate near the limits of resolution and depth penetration. As a result, diverse attempts have been made to enhance sensitivity to target features. Not all of these have been fully reproducible, and the overselling associated with overly optimistic conceptions has repeatedly discredited the EM method (e.g., Peters and Bardeen 1932; Constable 2010). Nevertheless, various approaches for sensitivity enhancement have been proposed on a reasonable physical basis.

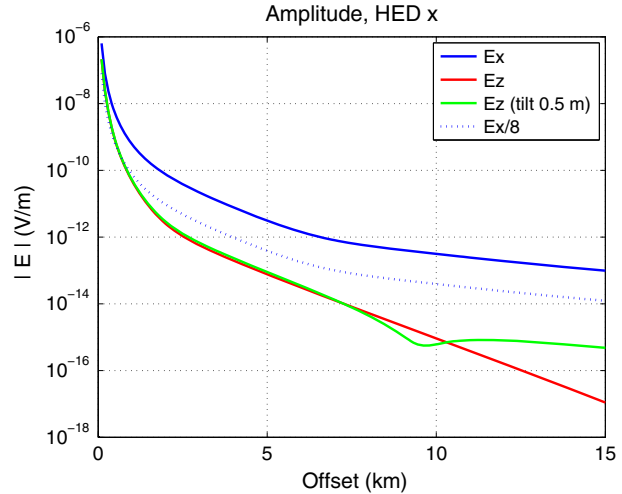
Methods looking at ratios between different field components or measurements at different locations, directions of polarization or tilt angle, or relations between fields at different frequencies were in use before quantitative interpretation of EM data became feasible (Frischknecht et al. 1991). Significant effort was made on perfecting such techniques, e.g., by developing dedicated systems for dual-frequency measurements (Johnson and Doborzynski 1986). Focusing approaches have also been considered more recently, based on ideas of taking differences between recordings made at different locations (Davydycheva and Rykhlini 2011) or frequencies (Maaø and Nguyen 2010), such that major signal components that contain little target information cancel out, or based on more general ideas of beamforming (Fan et al. 2012). Such approaches may enhance the signal under certain circumstances. However, they also bear the danger of enhancing noise and introducing artifacts when applied without sufficient caution, and if the structure to be focused on is not known to a sufficiently high degree of certainty. Such techniques may thus be beneficial for future monitoring applications, when small changes in a relatively well-known environment need to be detected.

3.4.1 Vertical Electric Sources and Receivers

Another obvious way of enhancing sensitivity is deploying instruments near the target structure, because features located in the vicinity of the sources and receivers influence measured responses most strongly. For surface measurements attempting to sense deep structure, high sensitivity to near-surface inhomogeneity is an undesired effect. Attempts have thus been made to mitigate the influence of near-source or near-receiver heterogeneity on recorded EM signal (Pellerin and Hohmann 1990; Hördt and Scholl 2004). We can exploit this effect, though, by placing sources or receivers in boreholes near the exploration target (e.g., Boyd and Wiles 1984). For electric sources and receivers, this will typically imply (nearly) vertical source or receiver geometries. Such geometries have the additional attractive property that they respond strongly to resistors (see Fig. 1e). This has also been shown in previous sensitivity studies (Pellerin and Hohmann 1995; Constable and Weiss 2006; Um and Alumbaugh 2007; Streich et al. 2010; Schaller et al. 2014) and is a result of the vertical electric field being free of modes traveling through air (Weidelt 2007a).

Although E_z is, in principle, more sensitive to resistive bodies than the horizontal electric field, measuring E_z poses practical problems. At the surface, amplitudes of E_z decrease to nearly zero. Measurements of E_z thus have to be made at some depth below the surface (or using long antennas in the air, yet this is likely to produce very noisy signal unless impractically massive installations are employed). Because E_z increases rapidly with depth, deploying sensors at shallow depth may be an economically feasible approach for recording useful E_z signal. In Fig. 6, amplitudes of E_z for vertical dipole sensors extending from 5 to 105 m depth are compared to amplitudes of the horizontal electric field

Fig. 6 Amplitudes of E_x for surface sensors, E_z for vertical dipoles extending from 5 to 105 m depth, and the electric field for near-vertical dipoles that extend over the same depth range and are tilted in the x direction by 0.5 m. Data are shown for the resistive layer model displayed in Fig. 1a and frequency 0.2 Hz. For comparison with the noise records in Fig. 8, E_x divided by eight is also shown



at the surface. This example shows that E_z amplitudes in such a scenario must be expected to be 10–100 times smaller than E_x amplitudes.

As deploying sensors perfectly vertically is difficult in practice, it is important to consider the influence of sensor tilt on vertical-field measurements. Because of the large amplitude differences between E_x and E_z , slight tilt, on the order of less than one degree, introduces significant horizontal components into the 'vertical' measurements that can result in amplitude changes by orders of magnitude (Fig. 6).

This is illustrated further in Fig. 7, in which E_z for 100-m-long exactly vertical sensors is compared to the near-vertical electric field for sensors that extend over 100 m vertically and are tilted in the x direction by 0.5 m (i.e., tilt angle 0.29°). At low frequencies and short offsets, the exactly and nearly vertical fields are similar. For tilted sensors, the amplitudes remain above the assumed noise floor of 10^{-15} V/(Am²) for higher frequencies and a wider offset range. Nevertheless, for the slight tilt considered here, the reservoir would be detectable within a similar frequency–distance range as for perfectly vertical sensors, with only a small shift toward lower frequencies (Fig. 7c, d). Also, the reservoir generates anomalies of similar strengths for the perfectly vertical and tilted sensors. This suggests that slight sensor tilt should not severely affect detectability of target structure, yet sensor orientation must be taken into account precisely during data inversion and interpretation. Analogously, Newman (1994) showed that, for borehole-to-surface measurements using a borehole source, target responses remained significant if the source was tilted, yet considering the exact source tilt was important for correct interpretation.

Unfortunately, noise levels of the horizontal and vertical electric field cannot be expected to decrease by the same ratio as signal levels. Measurements on the Arabian Peninsula (Colombo and McNeice 2013) and in Western Europe (Fig. 8) have found noise in E_z (or near-vertical recordings) to be roughly 5–8 times smaller than in the horizontal electric field. As a consequence, the source–receiver distance range in which the S/N ratio is sufficiently high for making useful observations is likely to be significantly smaller for E_z than for E_x and E_y . This implies that, to be able to make useful E_z observations, local conditions should be known prior to the survey more accurately than is required for

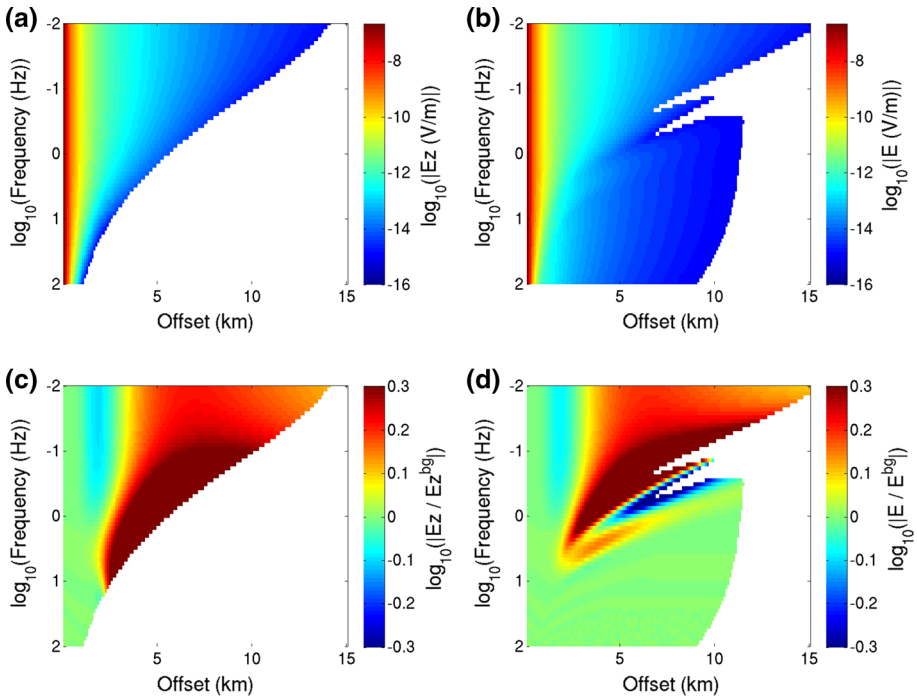


Fig. 7 **a** E_z and **b** the near-vertical electric field for sensors extending 100 m in depth and 0.5 m horizontally for the resistive layer model shown in Fig. 1a, and ratios of these fields to **c** E_z and **d** the near-vertical field for the corresponding background half-space model. Frequencies and distances at which either the resistive layer or background field falls below 10^{-15} V/m have been blanked

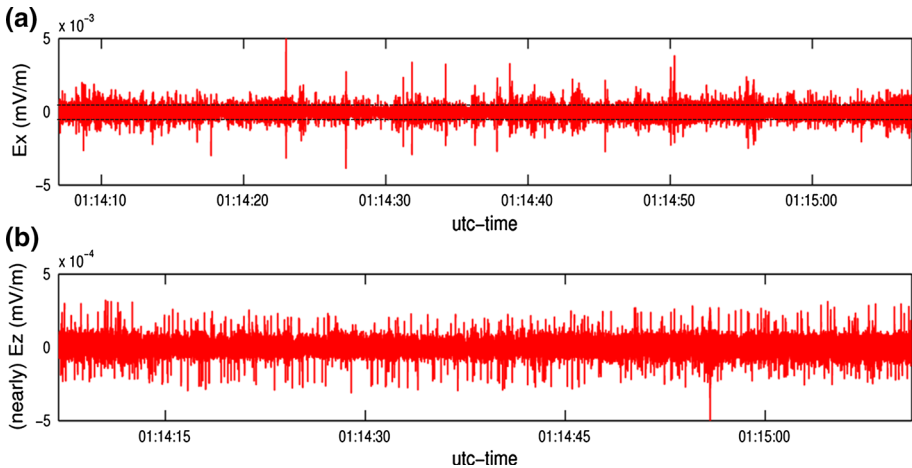


Fig. 8 Nighttime noise records from a site in the Netherlands of **a** the N-S-oriented horizontal electric field and **b** the near-vertical field at the same location, using an electrode dipole that extends from 5 to 100 m below the surface (deployed in direct contact with natural sediments without any well casing) and is horizontally tilted by 2.8 m. Data are sampled at (a) 500 Hz and (b) 512 Hz; power grid frequency of 50 Hz and its harmonics have been notch-filtered. *Dashed lines* in (a) indicate the amplitude scale of (b). Overall amplitudes in (b) are roughly 1/8 of those in (a)

horizontal field recording. Survey geometry needs to be tuned considering both subsurface illumination and signal-to-noise characteristics.

By reciprocity, similar sensitivity enhancement as from measuring E_z should be achievable by using vertical sources. These can be realized by placing source equipment in boreholes (He et al. 2005; Marsala et al. 2011; Cuevas 2012; Marsala et al. 2013; Cuevas 2014a) or using metallic wells casings as sources (Daily et al. 2004; Tietze and Ritter 2014; Hibbs et al. 2014). Alternatively, pseudo-vertical sources have been considered which use specific arrangements of equipment at the surface and specific current distributions to excite EM fields similar to those from vertical sources (Hall 1983; Mogilatov and Balashov 1996; Helwig et al. 2010). It remains to be seen for either of these approaches whether they will not only fulfill theoretical expectations regarding their imaging power, but also prove sufficiently robust and economically feasible to find wider practical application beyond trial experiments.

4 Dealing with Noise

Noise has complicated EM recording ever since the first EM measurements were made (Pettersson 1907). Szarka (1988) reviewed various types of noise that may contaminate EM data. Human-generated noise is emitted, as examples, by the power grid, power plants, railways, pipelines, industrial and agricultural facilities (factories, pumps, electric fences, etc.), or the mobile phone network. Large metallic bodies, such as well casings, can strongly alter EM field behavior locally. Instrument noise limits measurable EM field levels. Magnetotelluric signal is regarded as noise in the context of controlled-source EM surveying.

Earlier work was also concerned with geological noise, which was a synonym for subsurface features that influenced EM data, but were not considered in highly simplified (commonly 1D) subsurface models (Kaufman 1978; McCracken et al. 1986b; Kaufman 1989). This could be bodies at depth, small-scale structure near the sources or receivers not resolvable by the measurement technique used, or apparent anisotropy due to unresolvable small-scale features (Wannamaker 2005). Given the 3D modeling and interpretation capabilities available now, geological noise no longer needs to be termed “noise”. Instead, the search for just a single target body is being replaced by more comprehensive feasibility modeling and imaging that explicitly considers subsurface heterogeneity. Nevertheless, target responses can still be masked by responses from other nearby structure.

Further complications arise as EM exploration and monitoring work is commonly carried out in areas where numerous well casings are present. Strong influence of metallic well casings on EM records was recognized early and initially considered to render EM surveys useless in such areas (Karcher and McDermot 1935). Later studies attempted to quantify the currents induced into well casings and other elongated metallic objects such as pipelines (Wait 1972) in order to model their impact on EM data accurately (Wait 1952, 1983; Holladay and West 1984; Wait and Williams 1985; Wu and Habashy 1994; Pardo et al. 2008; Cuevas 2012; Swidinsky et al. 2013; Cuevas 2014b) and allow for subsurface interpretation in their presence.

4.1 Processing Techniques for Noise Reduction

The most important prerequisite for obtaining good signal-to-noise (S/N) ratios probably is making every possible effort to record high-quality data in the field. Nevertheless, noise-

reducing processing is invariably required. Various approaches have been proposed for enhancing S/N ratio in recorded EM data. Interpretable results have not always been obtained (Hördt et al. 2000), although most of the unsuccessful work likely has remained unpublished.

San Filippo and Hohmann (1983) numerically estimated the influence of MT signal on controlled-source data. They derived stacking requirements from their calculations and proposed using a remote reference for subtracting MT signal. Wilt et al. (1983) applied this technique and even report on using real-time telemetry for transmitting data from a remote-reference magnetometer. For most EM surveys today, MT signal likely is no longer the strongest source of noise. Rather, with electricity-generating and consuming facilities continually being expanded, man-made noise is an increasing problem. Such noise is local and may be correlated between different field components and nearby receivers, but its predictability between channels of a single station or nearby stations will be highly variable depending on local conditions. As a consequence, noise processing techniques that are successful for one survey may not easily be transferable to other sites, as can be seen, e.g., from the site-dependent success of Stephan and Strack (1991) with a noise reduction technique based on correlations between densely spaced receivers.

Ideas from MT processing have been adopted for cultural-noise processing. Macnae et al. (1984) describe data selection and weighting techniques that can improve S/N ratios beyond what can be achieved by simple stacking. Strack et al. (1989b) and Hanstein (1996) designed filters and selective stacking algorithms specifically for reducing noise in LOTEM data. Spies (1988) proposes noise prediction filters that attempt to estimate noise in vertical magnetic field transient EM records from horizontal field measurements at the same site.

Streich et al. (2013) adopt an MT processing approach for CSEM processing. They use a transmitter having three grounded electrodes through which three versions of a square wave or similar continuous source current, phase-shifted to one another by 120° , are fed into the ground. A bivariate relation is formulated between the source signal and recorded EM field, allowing to deconvolve source current waveforms using statistically robust weighted least-squares stacking algorithms known from MT processing. The result is Earth's impulse response functions in the frequency domain, for the frequency band contained in the source signal. Application of this processing scheme resulted in interpretable response functions for a CSEM data set collected across the CO₂ storage site at Ketzin, Germany (Fig. 9). These data were contaminated by strong noise from various sources, including several high-voltage power lines and cathodic protection currents that originated from a nearby gas pipeline and were several times stronger than the CSEM signal for some of the receivers.

4.2 Increasing the Source Moment

Another approach for elevating signal above noise levels is increasing the source strength. This can be achieved by increasing the source current, its size, or both. Experiments with sources of very high power (e.g., Keller et al. 1984; Freeman 1987), large dimensions (e.g., Zijl and Joubert 1975; Sternberg 1979; Velikhov et al. 2011; Barannik et al. 2013), or a combination of those (e.g., Velikhov et al. 1987; Zhdanov 2010) have been conducted repeatedly; see also a review describing large-source efforts by Boerner (1992). According to Ohm's law ($I = U/R$), high output current I can be achieved by using high source voltage U and/or lowering the system resistance R . Safety and cost considerations impose practical limitations on both U and R . For galvanically coupled sources, when relying on

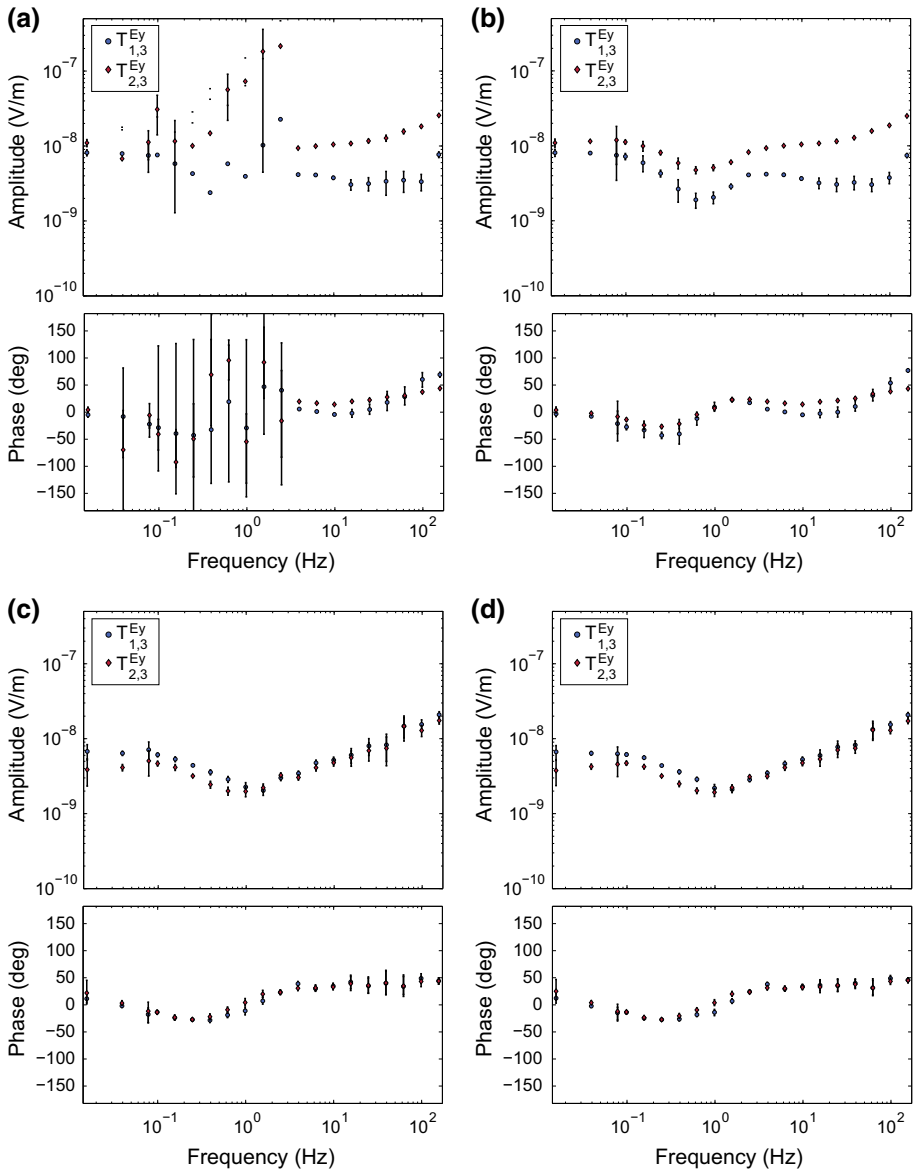


Fig. 9 Amplitudes and phases of response functions of noisy CSEM data collected in Germany. Shown are **a, b** data for a source–receiver distance of ~ 4.5 km acquired while strong pulsed cathodic protection currents (period 15 s) were fed into a pipeline passing the receiver at ~ 0.5 km distance, and **c, d** data for a source–receiver distance of ~ 7.5 km collected while currents on the pipeline were not pulsed. Results from simple least-squares stacking are displayed in **(a, c)**, and results from frequency-domain robust weighting in **(b, d)**. Adapted from Streich et al. (2013)

the voltage output of portable, widely available power generators, currents are inherently limited by the contact resistances of the source electrodes. For example, for a recently developed source that operates at a voltage of ~ 560 V (Streich et al. 2011), the nominal maximum output current of 40 A is only achieved if the sum of the contact resistances of

two source electrodes and the resistances of the electrode cables does not exceed $14\ \Omega$. Such low contact resistances are difficult and costly to achieve in arid, hard-rock, or permafrost environments, requiring large contact surfaces and/or deployment of electrodes into deeper, conductive units underneath resistive surface cover. Inductively coupled sources would eliminate this problem, yet lack sensitivity to resistive targets (see Fig. 1).

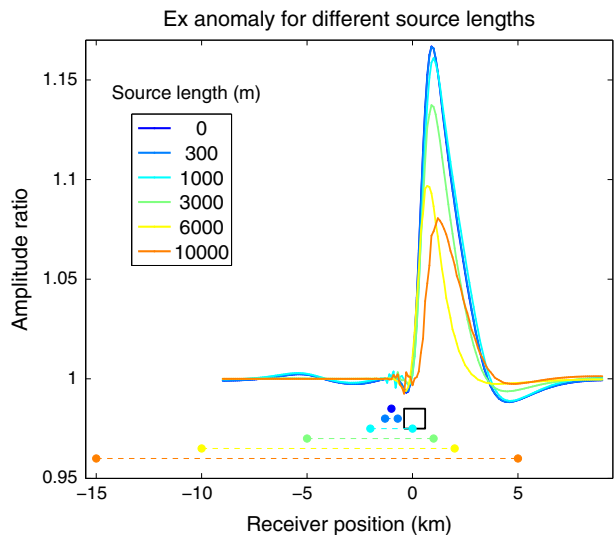
The option of maximizing source length has also been investigated. Zhamaletdinov et al. (2011) used industrial power lines more than 100 km long as source cables. They relate signal excited on the Kola Peninsula to recordings at distances up to more than 2000 km from the source, suggesting that controlled-source signal may, under exceptional circumstances, be detectable at very long distances. Nevertheless, suitable source sites are scarce. Also, source moments are distributed over the length of the source, and subsurface responses are integrated over long source–receiver offsets. As a result, the subsurface information retrievable from such recordings is of much lower resolution than required for resource exploration.

Even with sources of more moderate size, significant resolution can be lost in comparison with compact dipole sources. This is illustrated in Fig. 10, which shows electric field anomalies due to a resistive body of size $1 \times 1 \times 0.1$ km for an infinitesimal dipole and sources up to 10 km long. Long-source responses were calculated as described in Streich and Becken (2011). Lateral source positions were chosen such that target responses were maximized. For the infinitesimal dipole source, the target reservoir generates an anomaly of about 17 % in the inline electric field relative to the background field for a homogeneous half-space. With increasing source length, the anomaly decreases and is only about 7 % of the background field for a 10-km-long source.

4.3 Exploiting Noise as Signal

With cultural noise being abundant, the idea of trying to exploit the noise for subsurface imaging is obvious. This falls between passive EM techniques (MT) and techniques using fully controlled sources. Since such techniques may gain importance in the future, a few examples will be briefly described here.

Fig. 10 Inline electric field anomaly for a 3D target of resistivity $40\ \Omega\text{m}$ and dimensions $1 \times 1 \times 0.1$ km embedded in a $1.5\text{-}\Omega\text{m}$ half-space $0.7\text{--}0.8$ km below the surface, for an infinitesimal dipole source and source lengths up to 10 km (frequency 0.2 Hz). The dashed lines indicate the lateral positions of the sources. The *black box* indicates the lateral position of the target



Li and Pedersen (1991) and Qian and Pedersen (1991) derived MT-like impedances from noise originating from an industrial facility, which was located relatively far from the region surveyed, such that the noise could be shown to behave similarly to MT signal. Stray currents from electrified railways have long been known to generate noise (Schlumberger 1920). Whereas such noise has mostly been considered a nuisance to EM measurements (e.g., Fraser-Smith and Coates 1978), recent attempts have been made to use railway emissions. Neska (2009) and Tanbo et al. (2003) obtained approximate half-space resistivities from railway-generated EM data. Large parts of railway-generated signal are due to leakage currents flowing between the rail and ground (Lowes 2009). These currents depend in a complex fashion on local conditions (e.g., the layout of traction substations that supply currents to the railway system, the resistance between the rail and ground, train actions such as acceleration or braking). Because source characteristics are very difficult to determine precisely, ideas of treating the signal similarly to MT data have been investigated (Avdeeva et al. 2014).

In contrast, impressed-current cathodic protection systems of pipelines behave more similarly to controlled galvanic sources. Typically, currents of constant phase and period are fed into the pipelines at fixed points. Becken and Lindau (2014) test exploiting cathodic protection currents injected into pipelines for subsurface imaging, using current amplitudes measured along the pipeline for describing the source.

5 Data Interpretation

Our capability of quantitatively interpreting EM data has evolved somewhat slowly, lagging behind acquisition technology at various points in time. In the 1930s, EM fields could be measured, but not yet translated into subsurface resistivity (e.g., Statham 1936). Experiments with scale models fulfilled an important task of aiding interpretation when detailed numerical modeling still was beyond computational capabilities (Schlumberger 1920; Szarka 2009). Comparison of sounding curves of apparent resistivity to predetermined sets of type curves remained the standard way of interpretation from the 1960s well into the 1980s (Wait 1962; Goldstein and Strangway 1975; Spies and Frischknecht 1991). Apparent resistivity has been calculated from electric and magnetic field data or their combination, using near- or far-field, early- or late-time approximations. For example, Raiche (1983) derived apparent resistivity functions from measurements of the magnetic field and showed that this was advantageous over using measurements of its time derivative. Every apparent resistivity calculation approach has a limited range of validity and may produce artifacts that one must be careful with to avoid misinterpretation (Spies and Eggers 1986).

Fundamental insights on first-order field behavior, and apparent resistivity transforms, continue to be valuable for real-time quality assurance and quick initial interpretation. With gradual increase in computational power, this has been complemented by 1D inversion (e.g., Jupp and Vozoff 1975; Constable et al. 1987; Routh and Oldenburg 1999). Quite commonly, resistivity models constructed from stitched 1D inversions have been presented as the final results of EM surveys (e.g., Morrison et al. 1996; Ziolkowski et al. 2007; An and Di 2010; Antonov et al. 2014). This provides approximate subsurface images that sometimes are an acceptable compromise between accuracy and imaging cost. However, applying 1D interpretation to 3D structure may produce severe errors. Attempts have been made to quantify those errors (Gunderson et al. 1986; Nekut and Spies 1989)

and devise approximate correction procedures (Newman 1989). Results of 1D inversions can now be used for generating starting models for higher-dimensional inversion. Approximations such as the assumption of plane-wave fields in CSAMT continue to be used where appropriate for the targets and geological settings in question, yet are no longer strictly required in order to enable data interpretation.

Three-dimensional interpretation had been attempted long before computers were fully able to handle the required expensive calculations (Hohmann 1975; Pridmore et al. 1981). The achievement of 3D imaging was already mentioned as a point of major recent advance by Ward (1980). Nevertheless, 3D interpretation of large real data sets has only recently become widely available and practical for many EM practitioners, thanks to simultaneous advancements of computing power and modeling and imaging software. Modern laptop computers can now handle 3D simulations of moderate size, and cluster computing facilities have become widely accessible. Recently developed three-dimensional EM modeling codes (e.g., Weiss and Constable 2006; Streich 2009; Schwarzbach et al. 2011; Puzryev et al. 2013; Um et al. 2013) and imaging solutions (e.g., Haber et al. 2007; Gribenko and Zhdanov 2007; Commer and Newman 2008; Plessix and Mulder 2008; Commer and Newman 2009; Newman et al. 2010; Kumar et al. 2010; Schwarzbach and Haber 2013; Grayver et al. 2013; Oldenburg et al. 2013; Grayver et al. 2014) have matured to a point where they can be routinely employed by a wider user base. Newman (2014) reviews latest developments.

5.1 Integrated Interpretation of EM with Other Data

With the recent increased activity levels on multiphysics joint inversion (e.g., Stefano et al. 2011; Haber and Gazit 2013; Dell'Aversana 2014), it may seem as though data integration is a new idea. However, the importance of integrating EM with other data has long been recognized (e.g., Gish 1932; Andrieux 1996). Different EM techniques with complementary sensitivity properties have been combined in order to obtain more comprehensive subsurface images (e.g., Vozoff and Jupp 1975; Jupp and Vozoff 1977; Gómez-Trevino and Edwards 1983; Raiche et al. 1985; Meqbel and Ritter 2014; McMillan and Oldenburg 2014). Land and airborne EM data have been combined for enhancing spatial coverage from airborne data while taking advantage of the depth penetration and resolution of ground-based measurements (Sudha et al. 2014). In a sequential approach of utilizing different EM measurements, transient electromagnetic (TEM) data are commonly employed for static shift correction of MT data (Sternberg et al. 1988; Pellerin and Hohmann 1990; Árnason et al. 2010). EM and induced-polarization data have been jointly interpreted in surveys of potential hydrocarbon reservoirs (Dong et al. 2008; He et al. 2012).

Multiphysics integration of EM with other data has been done at multiple levels. Many of the recent examples consider marine settings, yet the integration strategies are equally valid for land data. Independent information from different geophysical methods can be joined at the interpretation stage (e.g., Harris and MacGregor 2006; Guerra et al. 2013). Independently obtained models of different geophysical parameters have been jointly inverted for petrophysical properties (Hoversten et al. 2006; Miotti et al. 2014). EM inversion can incorporate constraints such as information on seismic boundaries (Brown et al. 2012) or bodies (Lovatini et al. 2012). Cooperative inversion schemes have been devised that alternate between inversions of different data sets, each time using updated constraints (Um et al. 2014). Simultaneous joint inversion of multiphysics data (Stefano et al. 2011; Gallardo et al. 2012) attempts to reduce the non-uniqueness by searching for

linked models that fit the different data types. Further, attempts have been made to directly derive petrophysical parameters from joint inversion of EM and seismic data (Gao et al. 2012). In practice, it may be beneficial to use different integration approaches in sequence (Dell'Aversana 2014). Practical application examples of data integration include the use of EM to improve shallow seismic images (Mantovani et al. 2013; Colombo et al. 2013; Strack 2014), delineation of salt bodies (Moorkamp et al. 2013), or the definition of sub-basalt structure (Dell'Aversana et al. 2013). Recent reviews are provided by Gallardo and Meju (2011) and Haber and Gazit (2013).

6 EM Monitoring: The Future?

Monitoring has been highlighted as an area within which EM may find wider application in the future (e.g., Strack 2004, 2014). New cost-effective, high-resolution time-lapse EM techniques are being sought for various tasks, such as monitoring steam flooding of hydrocarbon reservoirs for enhanced oil recovery, or production of shale gas or oil requiring close monitoring of hydro-fracturing operations. In conventional hydrocarbon reservoirs, depleted and potentially bypassed volumes need to be identified. The propagation of carbon dioxide stored in the subsurface has to be monitored carefully. In all of these cases, technical and economic benefits of using EM will be evaluated against those of using other monitoring techniques, most prominently seismic, which has been applied successfully for reservoir monitoring (e.g., Greaves and Fulp 1987; Isaac and Lawton 2006; Kiyashchenko et al. 2013; Hornman and Forgues 2013).

Crucial requirements for monitoring obviously are sufficient accuracy and repeatability of the measurements, and sufficient sensitivity to the subsurface changes. Data errors have to be significantly smaller than the EM field changes resulting from changes within the target structure. Repeatability errors may be accumulated through repositioning errors of the acquisition equipment, hardware changes or aging, or temperature effects influencing hardware performance. Changes in water saturation may cause variations in near-surface resistivity and associated variations in equipment-to-ground coupling. General ambient noise levels may vary between surveys. Cultural-noise conditions may change due to changes in local infrastructure, installation of wind power plants, other industrial facilities, or electric fences. In producing fields, new wells may be drilled or new pipelines installed. Such large metallic bodies lead to current channeling and strong modifications of EM fields in their vicinity. In addition, uncertainties on background resistivity outside the changing reservoir may obscure the interpretation of time-lapse responses. Forward modeling codes generate data of limited accuracy. Errors originate from the discretization of Maxwell's equations as well as coarse approximate representations of actual resistivity structure. Further errors may be caused by limited accuracy of the linear system solver used.

6.1 Synthetic Studies

Numerous synthetic studies have investigated the feasibility of land EM monitoring. Water flooding of reservoirs constitutes a prime subject of interest (e.g., Rondeleux and Spitz 2010; Wirianto et al. 2010; Schamper et al. 2011; Colombo and McNeice 2013). Other synthetic studies consider the feasibility of monitoring resistivity changes related to CO₂ storage (Gasperikova and Hoversten 2006; Streich et al. 2010; Bourgeois and Girard 2010; Zhdanov et al. 2013; Vilamajó et al. 2013). Most of the synthetic studies investigate the

influence of noise and of some of the errors potentially affecting time-lapse data. For example, Schamper et al. (2011) study a case of water flooding of an oil reservoir, using borehole-to-surface measurement configurations. They demonstrate that, not surprisingly, time-lapse responses depend significantly on the resistivity structure outside the time-varying reservoir. Insufficient knowledge of the background resistivity may thus lead to misinterpretation of time-lapse responses, although, as also shown by Lien and Mannseth (2008), significant cancellation of erroneous assumptions on background resistivity can be expected. Measurable time-lapse changes of forward-modeled responses do not necessarily guarantee that volumes in which resistivity has changed will be correctly identified. Inversion of time-lapse data is quite likely to recover only part of the altered volume (Colombo and McNeice 2013; Zhdanov et al. 2013).

Almost without exception, published synthetic feasibility studies arrive at the conclusion that EM monitoring should, albeit marginally, be feasible. Nevertheless, there have not been many field applications of EM monitoring to date. The main cause of this discrepancy may lie in overly optimistic assumptions not being matched in practice. For example, idealized noise has been modeled as being random and dependent on controlled-source EM field amplitude (Wirianto et al. 2010). Correspondingly, optimistic measurability thresholds for time-lapse changes have been assumed. Wirianto et al. (2011) and Schamper et al. (2011) state that changes as small as 1 % of the EM field amplitude should be measurable. There also is a tendency to overestimate expected resistivity changes and sizes of affected volumes. For example, Rondeleux and Spitz (2010) show a best-case scenario with a resistivity change by a factor of 100, while mentioning that smaller changes should be investigated. Streich et al. (2010) present examples of time-lapse changes for a CO₂ injection scenario, where a resistive disk of 1 km diameter was considered to be able to visualize and study EM field behavior. They verified that the actual CO₂ volume in the underlying true injection experiment, which reached a diameter of roughly 300 m (Ivanova et al. 2012; Bergmann et al. 2014), would not have been detectable by surface-based CSEM measurements.

In many cases, resistivity changes have been grossly simplified by using homogenous blocks in which resistivity changes from one discrete value to another, although actual resistivity variations are known to be complex. Butler (1995) found from laboratory experiments that steam injection alters electrical conductivity in a complex fashion and may result in conductivity increase as well as decrease. Mansure et al. (1993) report similar findings from well-log data acquired before and after steam injection into several reservoirs.

Complex patterns of resistivity change are also indicated if resistivity is estimated based on reservoir simulation data. Figure 11 shows resistivity estimates for a heavy-oil reservoir

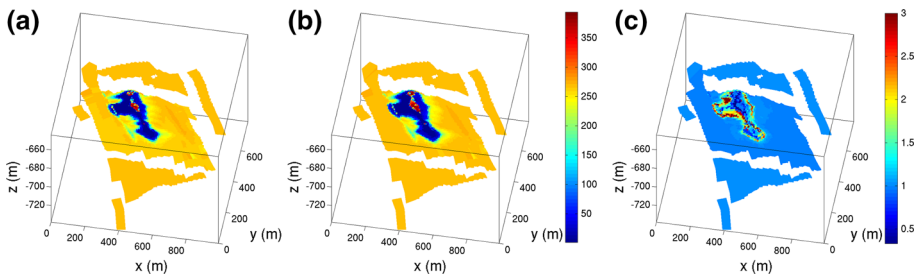


Fig. 11 Resistivity within an oil reservoir undergoing steam injection, estimated from reservoir simulation data and petrophysical relations. **a, b** Resistivity (Ωm) at two points in time, about 7 months apart. **c** The ratio between resistivities at the two times

undergoing gravity-assisted steam flooding. Baseline resistivity was taken from well-log data. Resistivity in the region affected by steam injection was calculated using oil, water and steam saturation, porosity, temperature, and salinity data from in situ measurements in observation wells and reservoir simulations. First, brine conductivity was estimated using a relation between salinity, temperature, and conductivity that is applicable over wide salinity and temperature ranges (Ucok et al. 1980). Then, resistivity of the non-shale fraction was calculated from Archie's law. Finally, the combined resistivity of the sand and shale fractions was estimated assuming a laminated shale model (Schön 2004). In the central part of the reservoir, near the injection well, resistivity increases above baseline values. Away from the injection well, resistivity decreases, as the steam gradually condenses, mixes with saline formation water, and displaces the highly resistive oil. Within a seven-month period, resistivity is predicted to increase somewhat near the injector and decrease near the edge of the volume influenced by the steam injection.

6.2 Monitoring Applications in Practice

Most of the scarce reported field applications of EM monitoring to date have been technology trials. For example, Bartel and Newman (1991) and Tseng et al. (1998) describe small-scale trials of injecting saline water into an aquifer at 30 m depth. Borehole-to-surface measurements were made to detect the salt water volume (Bartel and Newman 1991) and its removal from the subsurface (Tseng et al. 1998). DC monitoring demonstration studies have been carried out at somewhat larger scale, using cross-well (Tøndel et al. 2014) and borehole-to-surface (Bergmann et al. 2014) configurations. In a trial of MT monitoring of an enhanced geothermal system, significant changes of MT transfer functions were observed, and inferences could be made on the primary direction of fluid propagation (Peacock et al. 2013). He et al. (2015) interpret minor resistivity changes in a gas reservoir from time-lapse MT. In an experiment of TEM monitoring of steam injection, small observed changes in apparent resistivity were interpreted to coincide with steam flow patterns (Hu et al. 2008; He et al. 2010).

A prominent example of an EM monitoring trial is the attempt at delineating changes of gas content within an underground gas storage site (Hördt et al. 2000; Wright et al. 2002). The site was well suited for a monitoring test, because the reservoir is quite shallow (about 500 m) and resistivity between the gas-filled reservoir and the over- and underlying rocks differs by about an order of magnitude. Variations in response up to $\sim 5\%$ were expected (Hördt et al. 2000). Processing of repeat data acquired two years apart was first described by Hördt et al. (2000), in a rare and instructive publication of what was then considered disappointing results. Later reprocessing of the same data with additional calibration resulted in a more consistent-looking picture of time-lapse changes. These were interpreted to agree qualitatively with the seasonal variations of gas content in the reservoir (Wright et al. 2002).

There still is high uncertainty on the repeatability of EM measurements. Establishing repeatability errors is crucial for assessing EM monitoring feasibility in practice, yet published repeatability trials are scarce. One example, although marine, is Ziolkowski et al. (2010). After careful noise-reducing processing, they obtained average normalized RMS differences of 3.9 % between data collected one year apart, with part of these differences possibly related to changes within the reservoir surveyed. Tietze et al. (2015) obtain repeatability errors within 5 % for most of a land CSEM data set with recordings ten days apart, while part of their equipment was left in place between the two surveys. Such numbers appear large in view of the small impact of many features of interest on EM data;

in many cases, EM field changes due to changes within reservoirs must be expected to be of similar magnitude. Further effort on evaluating and improving repeatability is thus imperative.

To obtain large and reliable time-lapse responses, recent efforts have been focused on bringing instruments close to the targets and using borehole-to-surface configurations. Marsala et al. (2011) used a borehole-to-surface configuration with source electrodes deployed below the bottom of the casing and at the surface near the well. They managed to distinguish between water-flooded and oil-saturated regions within a reservoir, although the survey they reported on was a one-time experiment under favorable conditions with a fairly shallow reservoir and large expected resistivity contrasts. Cuevas (2014a) theoretically analyzes the behavior of a well casing used as an EM source, assuming that the current is injected into the casing through electrodes connected at its top and bottom. He finds that, for this configuration, anomalous bodies of moderate size should generate detectable EM field anomalies, similar to hypothetical anomalies generated when placing a source in a well without a casing. Several field trials of injecting currents into well casings have recently been run (Hibbs et al. 2014; Vilamajó et al. 2014; Tietze et al. 2015). Further effort is required to fully understand how currents are emitted from well casings into the ground and enable interpretation of such surveys to the level of accuracy necessary for EM monitoring.

7 Conclusions

Application of electromagnetic methods on land has a long and diverse history, extending way beyond the recent adoption of marine CSEM by the hydrocarbon industry. Land EM has been commercially most successful primarily in two domains. The first of these is mining applications, where resistivity contrasts between targets and host rocks commonly are large, and targets are more conductive than the host. The second one is well logging, where close correspondence between logged resistivity and hydrocarbon content can often be observed (although this is not always unambiguous; see, e.g., Gist et al. 2013). Nevertheless, numerous published examples provide evidence that land-based EM with man-made controlled sources has been applied continuously throughout the last century in the domain of hydrocarbon exploration. Limited use of EM in this domain can be attributed to limitations of sensitivity, resolution, penetration, noise, hardware. In many cases, those limitations make it physically infeasible to extract the information desired and, in some cases, they have inhibited successful surveys at a cost and effort justified by the amount of information gained.

In using EM for hydrocarbon exploration, we are typically faced with the task of imaging resistive reservoirs within a more conductive environment. Unfortunately, sensitivity of EM fields is such that this is considerably more difficult than the opposite task of imaging conductive bodies in a more resistive environment. For obtaining interpretable target responses, it is thus crucial to choose optimum source–receiver configurations and design surveys carefully. Nevertheless, if targets are too small, too deep, have too little contrast with the surroundings, or target responses are entirely masked by other subsurface features, it is important to honestly accept the physical limitations. This can prevent misuse and discreditation of EM methodology, as it was pointed out very sharply early on that “The quack and the shyster seem to have a strong predilection for electrical vestments” (Gish 1932).

For land EM acquisition systems, channel count even of reported recent multichannel systems (e.g., He et al. 2010) is still less than what would be desirable for 3D surveying. Therefore, EM practitioners today are still regularly faced with the choice between acquiring densely spaced profiles lacking 3D information, or too coarsely spaced 3D data. Certainly, acquisition geometries can be optimized for retrieving maximum amounts of information with minimum numbers of sources and receivers, if sufficient subsurface knowledge is available. Designing surveys with low channel count and thus minimum environmental impact also is important. Nevertheless, further instrumental developments are desirable that allow for easier deployment, make equipment more affordable, and thus facilitate more widespread use of multichannel systems and further increase in channel count. Denser sampling enables better quality control and allows us to interpret the unexpected subsurface features that must always be expected.

Increasing levels of cultural noise pose a severely growing challenge to land EM surveys. Future success of land EM applications may critically depend on improving the techniques for handling the various types of noise encountered. Methods for exploiting the noise explicitly by using it as source signal may gain importance. In other situations, the influence of noise may be reduced by recording field components less affected by noise or by defining source geometries and signals such that they are optimally separable from the noise. Further noise reduction may be achieved by developing advanced processing schemes that exploit some a priori knowledge of the noise at hand. Certain types of signal undesired at the outset, such as the effects of well casings, may have to be explicitly accounted for in data interpretation.

Thanks to simultaneous development of acquisition hardware, computers, processing, and modeling and inversion algorithms, we can now almost routinely produce 3D images of subsurface resistivity. The image quality achievable by the latest 3D modeling and inversion tools is probably approaching the fundamental physical limits of resolution. Resistivity images constructed from 1D inversion results are still seen quite commonly though; it would be desirable to make the latest cutting-edge imaging tools more widely accessible. Inherent ambiguity still remains in resistivity images, which is unlikely to be resolvable from EM data alone. Therefore, high expectations rightfully lie in further integration of EM with other data.

Land EM may find wider application for monitoring tasks in the future. Yet, despite the various past feasibility studies and few field trials, large-scale industry pickup has not yet occurred and may not occur before significant additional research work has been completed. Field trials are required to first establish and then lower repeatability thresholds. Survey configurations need to be implemented that possess sufficient sensitivity to the small resistivity changes to be monitored. In many cases, this is likely to require placing instruments at depths near the targets. Accordingly, we need to improve our understanding of borehole-to-surface configurations, particularly those that make use of well casings or are deployed at sites with casings present. Surveys using boreholes are laborious and expensive; it is thus also important to develop solutions that are cost-competitive with other (non-EM) technologies available for reservoir monitoring.

In trying to assess the future of EM monitoring, it is interesting to look back at a prediction on marine CSEM application for hydrocarbon exploration made in 1989: “Presently, there is limited motivation to develop seafloor CSEM methods for petroleum exploration applications due to the high cost of deploying seafloor instrumentation and due to the high quality and low cost of marine seismic data. It is likely that seafloor CSEM techniques will play an important role in studies of the oceanic lithosphere and in mineral exploration applications” (Nekut and Spies 1989). Only ten years later, marine CSEM was

adopted by the hydrocarbon industry. The future of land EM applications, for monitoring as well as exploration tasks, is equally unpredictable. Given the sensitivity of EM to a subsurface property not seen by other geophysical methods, and its capabilities proven to date, it certainly is desirable that onshore controlled-source EM not only retains its place as an integral part of the geophysical toolbox, but also be further developed to exploit it to its full potential.

Acknowledgments I would like to thank Oliver Ritter, Ian Ferguson, and the other members of the Program Committee of the 22nd EM Induction Workshop for giving me the opportunity to present and write this review, and Shell for permitting me to work on it. I am grateful for discussions with many colleagues over the years that have broadened and deepened my understanding of EM phenomena, and continue to do so. Constructive comments from two reviewers and the Associate Editor helped improve the manuscript.

References

- An Z, Di Q (2010) Application of the CSAMT method for exploring deep coal mines in Fujian Province, Southeastern China. *J Environ Eng Geophys* 15(4):243–249
- Andrieux P (1996) Introduction. *Geophys Prospect* 44(6):921–922
- Antonov EY, Kozhevnikov NO, Korsakov MA (2014) Software for inversion of TEM data affected by fast-decaying induced polarization. *Russ Geol Geophys* 55(8):1019–1027
- Árnason K, Eysteinnsson H, Hersir GP (2010) Joint 1D inversion of TEM and MT data and 3D inversion of MT data in the Hengill area, SW Iceland. *Geothermics* 39(1):13–34
- Avdeeva A, Becken M, Streich R (2014) Towards imaging the earth using EM fields emitted by DC railways. In: IAGA WG 1.2 workshop on electromagnetic induction in the earth, Weimar, Germany
- Barannik MB, Kolobov VV, Selivanov VN, Kuklin DV, Zhamaletdinov AA, Shevtsov AN (2013) Portable generator for deep electromagnetic soundings and monitoring of seismically active zones with the use of industrial power transmission lines. *Seism Instrum* 49(3):275–284
- Bartel LC, Newman GA (1991) Mapping a 3D conductivity anomaly using a vertical electric source: field results. In: SEG technical program expanded abstracts 1991, pp 472–475
- Becken M, Lindau T (2014) Utilizing impressed current cathodic protection as the source for electromagnetic exploration. In: 76th EAGE conference and exhibition—workshops, pp WS9–C06
- Bellairs G (1955) Instrumentation for a new electromagnetic geophysical field technique, as applied in South Africa. *Geophysics* 20(1):155–162
- Bergmann P, Ivandic M, Norden B, Rücker C, Kiessling D, Lüth S, Schmidt-Hattenberger C, Juhlin C (2014) Combination of seismic reflection and constrained resistivity inversion with an application to 4D imaging of the CO₂ storage site, Ketzin, Germany. *Geophysics* 79(2):B37–B50
- Blau LW (1933) Method and apparatus for geophysical exploration. United States Patent 1,911,137
- Blau LW, Statham L (1939) Electric earth transient in geophysical prospecting. United States Patent 2,160,824
- Blau LW, Statham L (1940) Electric earth transients in geophysical prospecting. United States Patent 2,202,369
- Boerner DE (1992) Controlled source electromagnetic deep sounding: theory, results and correlation with natural source results. *Surv Geophys* 13(4–5):435–488
- Bourgeois B, Girard J (2010) First modelling results of the EM response of a CO₂ storage in the Paris Basin. *Oil Gas Sci Technol Rev IFP* 65(4):597–614
- Boyd GW, Wiles CJ (1984) The Newmont drillhole EMP system—examples from eastern Australia. *Geophysics* 49(7):949–956
- Brown V, Key K, Singh S (2012) Seismically regularized controlled-source electromagnetic inversion. *Geophysics* 77(1):E57–E65
- Butler DB (1995) The effect of steam injection on the electrical conductivity of sand and clay. Ph.D. thesis, University of British Columbia
- Chave AD (2009) On the electromagnetic fields produced by marine frequency domain controlled sources. *Geophys J Int* 179:1429–1457
- Chen J, Alumbaugh DL (2011) Three methods for mitigating airwaves in shallow water marine controlled-source electromagnetic data. *Geophysics* 76(2):F89–F99
- Colombo D, McNeice GW (2013) Quantifying surface-to-reservoir electromagnetics for waterflood monitoring in a Saudi Arabian carbonate reservoir. *Geophysics* 78(6):E281–E297

- Colombo D, Rovetta D, Sandoval Curiel E, Ley RE, Wang W, Liang C (2013) 3D seismic-gravity simultaneous joint inversion for near surface velocity estimation. In: 75th EAGE conference and exhibition, London, p Th 01 06
- Commer M, Newman GA (2008) New advances in three-dimensional controlled-source electromagnetic inversion. *Geophys J Int* 172:513–535
- Commer M, Newman GA (2009) Three-dimensional controlled-source electromagnetic and magnetotelluric joint inversion. *Geophys J Int* 178(3):1305–1316
- Constable S (2010) Ten years of marine CSEM for hydrocarbon exploration. *Geophysics* 75(5):75A67–75A81
- Constable S, Weiss CJ (2006) Mapping thin resistors and hydrocarbons with marine EM methods: insights from 1D modeling. *Geophysics* 71(2):G43–G51
- Constable SC, Parker RL, Constable CG (1987) Occam's inversion: a practical algorithm for generating smooth models from electromagnetic sounding data. *Geophysics* 75(3):289–300
- Cuevas N (2012) Casing effect in borehole-surface (surface-borehole) EM fields. In: 74th EAGE conference, Barcelona, extended abstract, p P201
- Cuevas N (2014a) Energizing a bipole casing electromagnetic source—sensitivity analysis. In: 76th EAGE conference, Amsterdam, extended abstract, p We E108 01
- Cuevas NH (2014b) Analytical solutions of EM fields due to a dipolar source inside an infinite casing. *Geophysics* 79(5):E231–E241
- Daft L, Williams A (1906) Apparatus for detecting and localizing mineral deposits. US Patent 817,736
- Daily W, Ramirez A, Newmark R, Masica K (2004) Low-cost reservoir tomographs of electrical resistivity. *Lead Edge* 23(5):472–480
- Davydycheva S (2010) 3D modeling of new-generation (1999–2010) resistivity logging tools. *Lead Edge* 29(7):780–789
- Davydycheva S, Rykhlini N (2011) Focused-source electromagnetic survey versus standard CSEM: 3D modeling in complex geometries. *Geophysics* 76(1):F27–F41
- De Stefano M, Golfre Andreasi F, Re S, Virgilio M, Snyder FF (2011) Multiple-domain, simultaneous joint inversion of geophysical data with application to subsalt imaging. *Geophysics* 76(3):R69–R80
- Dell'Aversana P (2014) Integrated geophysical models—combining rock physics with seismic, electromagnetic and gravity data. EAGE Publications BV, Houten
- Dell'Aversana P, Ravasio A, Vitale S, Bernasconi G (2013) An integrated geophysical approach for sub basalt exploration. In: 75th EAGE conference and exhibition, London, p We 04 01
- Dong W, Zhao X, Liu F, Zhao G (2008) The time-frequency electromagnetic method and its application in western China. *Appl Geophys* 5(2):127–135
- Druskin VL, Knizhnerman LA (1988) A spectral finite-difference method for numerical-solution of three-dimensional nonstationary problems in electrical prospecting. *Izvestiya Akademii Nauk SSSR, Fizika Zemli* 8:63–74 in Russian
- Duckworth K, O'Neill D (1989) Detection of a brine conductor under an oil field by means of a fixed transmitter electromagnetic survey using a SQUID magnetometer. *Can J Explor Geophys* 25(1):61–73
- Duncan PM, Hwang A, Edwards RN, Bailey RC, Garland GD (1980) The development and applications of a wide band electromagnetic sounding system using a pseudo-noise source. *Geophysics* 45(8):1276–1296
- Eadie T (1980) Detection of hydrocarbon accumulations by surface electrical methods: a feasibility study. Master's thesis, University of Toronto
- Eidesmo T, Ellingsrud S, MacGregor LM, Constable S, Sinha MC, Johansen S, Kong FN, Westerdahl H (2002) Sea Bed Logging (SBL), a new method for remote and direct identification of hydrocarbon filled layers in deepwater areas. *First Break* 20(3):144–152
- Ellingsrud S, Eidesmo T, Sinha MC, MacGregor LM, Constable S (2002) Remote sensing of hydrocarbon layers by Seabed Logging (SBL): results from a cruise offshore Angola. *Lead Edge* 21(10):972–982
- Enslin JF (1955) A new electromagnetic field technique. *Geophysics* 20(2):318–334
- Everett ME (2012) Theoretical developments in electromagnetic induction geophysics with selected applications in the near surface. *Surv Geophys* 33(1):29–63
- Fan Y, Snieder R, Slob E, Hunziker J, Singer J, Sheiman J, Rosenquist M (2012) Increasing the sensitivity of controlled-source electromagnetics with synthetic aperture. *Geophysics* 77(2):E135–E145
- Fox RW (1830) On the electro-magnetic properties of metalliferous veins in the mines of Cornwall. *Philos T R Soc Lond* 120(B3):399–414
- Fraser-Smith AC, Coates DB (1978) Large-amplitude ULF electromagnetic fields from BART. *Radio Sci* 13(4):661–668
- Freeman M (1987) MHD pulsed power for geophysics and the SDI. *Exec Intell Rev* 14(7):24–31
- Frischknecht FC, Raab PV (1984) Time-domain electromagnetic soundings at the Nevada Test Site, Nevada. *Geophysics* 49(7):981–992

- Frisknecht FC, Labson VF, Spies BR, Anderson WL (1991) Profiling methods using small sources. In: Nabighian MN (ed) *Electromagnetic methods in applied geophysics*, vol 2. Society of Exploration Geophysicists, Tulsa, pp 105–270
- Gallardo LA, Fontes SL, Meju MA, Buonora MP, de Lugao PP (2012) Robust geophysical integration through structure-coupled joint inversion and multispectral fusion of seismic reflection, magnetotelluric, magnetic, and gravity images: example from Santos Basin, offshore Brazil. *Geophysics* 77(5):B237–B251
- Gallardo LA, Meju MA (2011) Structure-coupled multiphysics imaging in geophysical sciences. *Rev Geophys* 49(1):1–19
- Gao G, Abubakar A, Habashy TM (2012) Joint petrophysical inversion of electromagnetic and full-waveform seismic data. *Geophysics* 77(3):WA3–WA18
- Gasperikova E, Hoversten GM (2006) A feasibility study of nonseismic geophysical methods for monitoring geologic CO₂ sequestration. *Lead Edge* 25(10):1282–1288
- Gella N (1930) Geo-electric investigations of non-conductors: four new examples. *AAPG Bull* 14(9):1165–1176
- Gish OH (1932) Use of geoelectric methods in search for oil. *AAPG Bull* 16(12):1337–1348
- Gist G, Ciucivara A, Houck R, Rainwater M, Willen D, Zhou J-J (2013) Case study of a CSEM false positive—Orphan Basin, Canada. In: Society of Exploration Geophysicists annual meeting, expanded abstract, Houston, pp 805–809
- Glenn WE, Ryu J, Ward SH, Peeples WJ, Phillips RJ (1973) The inversion of vertical magnetic dipole sounding data. *Geophysics* 38(6):1109–1129
- Goldstein MA, Strangway DW (1975) Audio-frequency magnetotellurics with a grounded electric dipole source. *Geophysics* 40(4):669–683
- Gómez-Trevino E, Edwards RN (1983) Electromagnetic soundings in the sedimentary basin of southern Ontario—a case history. *Geophysics* 48(3):311–330
- Gómez-Treviño E, Esparza FJ (2014) What is the depth of investigation of a resistivity measurement? *Geophysics* 79(2):W1–W10
- Grayver AV, Streich R, Ritter O (2014) 3D inversion and resolution analysis of land-based CSEM data from the Ketzin CO₂ storage formation. *Geophysics* 79(2):E101–E114
- Grayver AV, Streich R, Ritter O (2013) Three-dimensional parallel distributed inversion of CSEM data using a direct forward solver. *Geophys J Int* 193:1432–1446
- Greaves RJ, Fulp TJ (1987) Threedimensional seismic monitoring of an enhanced oil recovery process. *Geophysics* 52(9):1175–1187
- Gribenko A, Zhdanov M (2007) Rigorous 3D inversion of marine CSEM data based on the integral equation method. *Geophysics* 72(2):WA73–WA84
- Guelke R (1945) A geophysical prospecting instrument using alternating currents of audio-frequency. *J Sci Instrum* 22(8):141–145
- Guerra I, Ceci F, Miotti F, Lovatini A, Milne G, Paydayesh M, Leathard M, Sharma A (2013) Multi-measurement integration—a case study from the Barents Sea. *First Break* 31(4):55–61
- Gunderson BM, Newman GA, Hohmann GW (1986) Threedimensional transient electromagnetic responses for a grounded source. *Geophysics* 51(11):2117–2130
- Haber E, Gazit MH (2013) Model fusion and joint inversion. *Surv Geophys* 34:675–695
- Haber E, Oldenburg DW, Shekhtman R (2007) Inversion of time domain three-dimensional electromagnetic data. *Geophys J Int* 171:550–564
- Hall SH (1983) The rotating current dipole. *Geophysics* 48(9):1233–1247
- Hanstein T (1996) Digitale Optimalfilter für LOTEM Daten. In: *Protokoll über das Kolloquium Elektromagnetische Tiefenforschung*, pp 320–328
- Harris P, MacGregor L (2006) Determination of reservoir properties from the integration of CSEM, seismic, and well-log data. *First Break* 24(11):53–59
- He Z, Hu W, Dong W (2010) Petroleum electromagnetic prospecting advances and case studies in China. *Surv Geophys* 31(2):207–224
- He Z, Hu Z, Gao Y, He L, Meng C, Yang L (2015) Field test of monitoring gas reservoir development using time-lapse continuous electromagnetic profile method. *Geophysics* 80(2):WA127–WA134
- He Z, Liu X, Qiu W, Zhou H (2005) Mapping reservoir boundary by borehole-surface TFEM: two case studies. *Lead Edge* 24(9):896–900
- He Z, Zhao Z, Liu H, Qin J (2012) TFEM for oil detection: case studies. *Lead Edge* 31(5):518–521
- Hedstrom H (1930) Electrical survey of structural conditions in Salt Flat field, Caldwell County, Texas. *AAPG Bull* 14(9):1177–1185
- Heiland CA (1932) Advances in technique and application of resistivity and potential-drop-ratio methods in oil prospecting. *AAPG Bull* 16(12):1260–1336

- Helwig SL (1998) Using PRBS-sequences as source for TEM-measurements. In: 60th EAGE conference, Leipzig, extended abstract
- Helwig SL, Mogilatov VS, Balashov BP (2010) Enhanced sensitivity in land EM by using an unconventional source. In: EGM international workshop, Capri, Italy, extended abstract
- Hestenes MR, Stiefel E (1952) Methods of conjugate gradients for solving linear systems. *J Res Natl Bur Stand* 49(6):409–436
- Hibbs AD, Petrov TR, Pendleton J, Agundes A, Kouba S, Hall T, Boyle D, Martin T, Schenkel C, Morrison HF (2014) Advances in electromagnetic survey instrumentation and the use of a cased borehole for imaging a deep formations. In: 76th EAGE conference and exhibition—workshops, pp WS9–C05
- Hohmann GW (1975) Three-dimensional induced polarization and electromagnetic modeling. *Geophysics* 40(2):309–324
- Hohmann GW, Vanvoorhis GD, Nelson PH (1978) A vector EM system and its field applications. *Geophysics* 43(7):1418–1440
- Holladay JS, West GF (1984) Effect of well casings on surface electrical surveys. *Geophysics* 49(2):177–188
- Hördt A, Andrieux P, Neubauer F, Rüter H, Vozoff K (2000) A first attempt at monitoring underground gas storage by means of time-lapse multichannel transient electromagnetics. *Geophys Prospect* 48:489–509
- Hördt A, Scholl C (2004) The effect of local distortions on timedomain electromagnetic measurements. *Geophysics* 69(1):87–96
- Hornman K, Forgues E (2013) Permanent reservoir monitoring with onshore surface seismic. In: Second EAGE workshop on permanent reservoir monitoring, pp We–01–04
- Hoversten GM, Cassassuce F, Gasperikova E, Newman GA, Chen J, Rubin Y, Hou Z, Vasco D (2006) Direct reservoir parameter estimation using joint inversion of marine seismic AVA and CSEM data. *Geophysics* 71(3):C1–C13
- Hu W, Yan L, Su Z, Zheng R, Strack K (2008) Array TEM sounding and application for reservoir monitoring. In: SEG technical program expanded abstracts, pp 634–638
- Hughes LJ, Carlson NR (1987) Structure mapping at Trap Spring Oilfield, Nevada, using controlled-source magnetotellurics. *First Break* 5(11):403–418
- Isaac JH, Lawton DC (2006) A case history of time-lapse 3D seismic surveys at Cold Lake, Alberta, Canada. *Geophysics* 71(4):B93–B99
- Ivanova A, Kashubin A, Juhojuntti N, Kummerow J, Henniges J, Juhlin C, Lüth S, Ivandic M (2012) Monitoring and volumetric estimation of injected CO₂ using 4D seismic, petrophysical data, core measurements and well logging: a case study at Ketzin, Germany. *Geophys Prospect* 60(5):957–973
- Jenny WP (1930) Electric and electromagnetic prospecting for oil. *AAPG Bull* 14(9):1199–1213
- Johnson IM, Doborzynski ZB (1986) A novel ground electromagnetic system. *Geophysics* 51(2):396–409
- Jupp DLB, Vozoff K (1975) Stable iterative methods for the inversion of geophysical data. *Geophys J R Astr S* 42(3):957–976
- Jupp DLB, Vozoff K (1977) Resolving anisotropy in layered media by joint inversion. *Geophys Prospect* 25(3):460–470
- Karcher JC, McDermot E (1935) Deep electrical prospecting. *AAPG Bull* 19(1):64–77
- Kaufman AA (1978) Resolving capabilities of the inductive methods of electroprospecting. *Geophysics* 43(7):1392–1398
- Kaufman AA (1989) A paradox in geoelectromagnetism, and its resolution, demonstrating the equivalence of frequency and transient domain methods. *Geoexploration* 25(4):287–317
- Kaufman AA, Alekseev D, Oristaglio M (2014) Principles of electromagnetic methods in surface geophysics. In: *Methods in geochemistry and geophysics*, vol 45. Elsevier, Amsterdam
- Kaufman AA, Dashevsky YA (2003) Principles of induction logging. In: *Methods in geochemistry and geophysics*, vol 38. Elsevier, Amsterdam
- Kaufman AA, Keller CV (1983) Frequency and transient soundings. Elsevier, Amsterdam
- Keller GV, Frischknecht FC (1966) Electrical methods of geophysical prospecting. Pergamon, Elmsford
- Keller GV, Pritchard JJ, Jacobson JJ, Harthill N (1984) Megasource timedomain electromagnetic sounding methods. *Geophysics* 49(7):993–1009
- Kiyashchenko D, Lopez J, Berlang W, Birch B, Zwaan M, Adawi R, Rocco G, Ghafri S (2013) Steam-injection monitoring in South Oman—from single-pattern to field-scale surveillance. *Lead Edge* 32(10):1246–1256
- Kumar R, Al-Saeed MA, Khalid A, Lovatini A, Pezzoli M, Battaglini A, Ceci F, Roth J (2010) Land controlled-source electromagnetic surveying for viscous oil characterization in Kuwait. In: 75th EAGE conference, London, extended abstract, p We 04 06
- Li X, Pedersen LB (1991) Controlled source tensor magnetotellurics. *Geophysics* 56(9):1456–1461

- Lien M, Mannseth T (2008) Sensitivity study of marine CSEM data for reservoir production monitoring. *Geophysics* 73(4):F151–F163
- Løseth LO, Amundsen L, Jenssen AJK (2010) A solution to the airwave-removal problem in shallow-water marine EM. *Geophysics* 75(5):A37–A42
- Lovatini A, Medina E, Pezzoli M (2012) Seismic geobody-driven 3D controlled-source electromagnetic modeling. In: 74th EAGE conference, Copenhagen, extended abstract, p A012
- Lowes FJ (2009) DC railways and the magnetic fields they produce—the geomagnetic context. *Earth Planets Space*, 61:i–xv
- Maaø FA, Nguyen AK (2010) Enhanced subsurface response for marine CSEM surveying. *Geophysics* 75(3):A7–A10
- MacGregor L, Andreis D, Tomlinson J, Barker N (2006) Controlled-source electromagnetic imaging on the Nuggets-1 reservoir. *Lead Edge* 25(8):984–992
- Macnae J, Lamontagne Y, West G (1984) Noise processing techniques for timedomain em systems. *Geophysics* 49(7):934–948
- Maillet R (1947) The fundamental equations of electrical prospecting. *Geophysics* 12(4):529–556
- Mansure AJ, Meldau RF, Weyland HV (1993) Field examples of electrical resistivity changes during steamflooding. *SPE Form Eval* 8(1):57–64
- Mantovani M, Clementi M, Ceci F (2013) Use of simultaneous joint inversion as a maximum concordance solver for statics. In: 75th EAGE conference and exhibition, London, p Th–01–03
- Marsala AF, Al-Buali M, Ali Z, Ma SM, He Z, Biyan T, He T, Zhao G (2011) First pilot of borehole to surface electromagnetic in Saudi Arabia—a new technology to enhance reservoir mapping and monitoring. In: 73rd EAGE conference and exhibition, Vienna, Austria, p 1005
- Marsala AF, Lyngra S, Widjaja DR, Laota AS, Al-Otaibi NM, He Z, Zhao G, Xu J, Yang C (2013) Fluid distribution inter-well mapping in multiple reservoirs by innovative borehole to surface electromagnetic: survey design and field acquisition. In: International petroleum technology conference (IPTC), Beijing, China, p IPTC 17045
- McBarnet A, Ziolkowski A (2005) Why MTEM sounded a good idea at the time. *First Break* 23(1):59–62
- McCracken KG, Oristaglio ML, Hohmann GW (1986a) A comparison of electromagnetic exploration systems. *Geophysics* 51(3):810–818
- McCracken KG, Oristaglio ML, Hohmann GW (1986b) Minimization of noise in electromagnetic exploration systems. *Geophysics* 51(3):819–832
- McCracken K G, Hohmann GW, Oristaglio ML (1980) Why time domain?: The geophysics of the Elura Orebody, Cobar, NSW. In Emerson DW (ed) Proceedings of the ELURA symposium, Sydney, Australia. Australian Society of Exploration Geophysicists, pp 176–179
- McMillan MS, Oldenburg DW (2014) Cooperative constrained inversion of multiple electromagnetic data sets. *Geophysics* 79(4):B173–B185
- Melton BS (1937) Electromagnetic prospecting method. United States Patent 2,077,707
- Meqbel N, Ritter O (2014) New advances for a joint 3D inversion of multiple EM methods. In: 76th EAGE conference and exhibition—workshops, pp WS9–B03
- Miotti F, Guerra I, Ceci F, Lovatini A, Paydayesh M, Milne G, Leathard M, Sharma A (2014) Estimation of the petrophysical model through the joint inversion of seismic and EM attributes. In: 76th EAGE conference and exhibition—workshops, pp WS9–B04
- Mogilatov V, Balashov B (1996) A new method of geoelectrical prospecting by vertical electric current soundings. *J Appl Geophys* 36:31–41
- Moorkamp M, Roberts AW, Jegen M, Heincke B, Hobbs RW (2013) Verification of velocity–resistivity relationships derived from structural joint inversion with borehole data. *Geophys Res Lett* 40:1–6
- Morrison HF, Shoham Y, Hoversten GM, Torres-Verdín C (1996) Electromagnetic mapping of electrical conductivity beneath the Columbia basalts. *Geophys Prospect* 44(6):963–986
- Muñoz G (2014) Exploring for geothermal resources with electromagnetic methods. *Surv Geophys* 35(1):101–122
- Nabighian M (2012) Comment on electromagnetic geophysics: notes from the past and the road ahead (Michael S Zhdanov, 2010, *Geophysics*, 75, no. 5, 75A4975A66). *Geophysics* 77(4):X3–X10
- Nabighian MN (1979) Quasistatic transient response of a conducting halfspace—an approximate representation. *Geophysics* 44(10):1700–1705
- Nabighian MN (ed) (1988) *Electromagnetic methods in applied geophysics*. In: Volume 1, Theory. Society of Exploration Geophysicists, Tulsa
- Nabighian MN (ed) (1991) *Electromagnetic methods in applied geophysics*. In: Volume 2, Application. Society of Exploration Geophysicists, Tulsa

- Nabighian MN, Macnae JC (1991) Time-domain electromagnetic prospecting methods. In: Nabighian MN (ed) *Electromagnetic methods in applied geophysics*, vol 2. Society of Exploration Geophysicists, Tulsa, pp 427–520
- Nekut AG, Spies BR (1989) Petroleum exploration using controlled-source electromagnetic methods. *Proc IEEE* 77(2):338–362
- Neska A (2009) Subsurface conductivity obtained from DC railway signal propagation with a dipole model. In: Ritter O, Weckmann U (eds) *Protokoll über das 23. Schmucker-Weidelt-Kolloquium für Elektromagnetische Tiefenforschung*. German Geophysical Society, Potsdam, pp 244–251
- Newman GA (1989) Deep transient electromagnetic soundings with a grounded source over near-surface conductors. *Geophys J Int* 98(3):587–601
- Newman GA (1994) A study of downhole electromagnetic sources for mapping enhanced oil recovery processes. *Geophysics* 59(4):534–545
- Newman GA (2014) A review of high-performance computational strategies for modeling and imaging of electromagnetic induction data. *Surv Geophys* 35(1):85–100
- Newman GA, Alumbaugh DL (1997) Three-dimensional massively parallel electromagnetic inversion—I. Theory. *Geophys J Int* 128:345–354
- Newman GA, Commer M, Carazzone JJ (2010) Imaging CSEM data in the presence of electrical anisotropy. *Geophysics* 75(2):F51–F61
- Oldenburg DW, Haber E, Shekhtman R (2013) Three dimensional inversion of multisource time domain electromagnetic data. *Geophysics* 78(1):E47–E57
- Oristaglio M, Worthington M (1980) Inversion of surface and borehole electromagnetic data for two-dimensional electrical conductivity models. *Geophys Prospect* 28(4):633–657
- Pardo D, Torres-Verdín C, Zhang Z (2008) Sensitivity study of borehole-to-surface and crosswell electromagnetic measurements acquired with energized steel casing to water displacement in hydrocarbon-bearing layers. *Geophysics* 73(6):F261–F268
- Passalacqua H (1983) Electromagnetic fields due to a thin resistive layer. *Geophys Prospect* 31(6):945–976
- Peacock JR, Thiel S, Heinson GS, Reid P (2013) Time-lapse magnetotelluric monitoring of an enhanced geothermal system. *Geophysics* 78(3):B121–B130
- Pellerin L, Hohmann GW (1990) Transient electromagnetic inversion: a remedy for magnetotelluric static shifts. *Geophysics* 55(9):1242–1250
- Pellerin L, Hohmann GW (1995) A parametric study of the vertical electric source. *Geophysics* 60(1):43–52
- Peters LJ, Bardeen J (1932) Some aspects of electrical prospecting applied in locating oil structures. *J Appl Phys* 2(3):103–122
- Petersson W (1907) Das Aufsuchen von Erzen mittels Elektrizität. *Glückauf* 43(29):906–910
- Plessix R-E, Darnet M, Mulder WA (2007) An approach for 3D multisource, multifrequency CSEM modeling. *Geophysics* 72(5):SM177–SM184
- Plessix R-E, Mulder WA (2008) Resistivity imaging with controlled-source electromagnetic data: depth and data weighting. *Inverse Probl* 24:034012
- Pridmore DF, Hohmann GW, Ward SH, Sil WR (1981) An investigation of finite-element modeling for electrical and electromagnetic data in three dimensions. *Geophysics* 46(7):1009–1024
- Puzirev V, Koldan J, de la Puente J, Houzeaux G, Vázquez M, Cela JM (2013) A parallel finite-element method for three-dimensional controlled-source electromagnetic forward modelling. *Geophys J Int* 193(2):678–693
- Qian W, Pedersen LB (1991) Industrial interference magnetotellurics: an example from the Tangshan area, China. *Geophysics* 56(2):265–273
- Raiche AP (1983) Comparison of apparent resistivity functions for transient electromagnetic methods. *Geophysics* 48(6):787–789
- Raiche AP, Jupp DLB, Rutter H, Vozoff K (1985) The joint use of coincident loop transient electromagnetic and Schlumberger sounding to resolve layered structures. *Geophysics* 50(10):1618–1627
- Rondeleux B, Spitz S (2010) Feasibility of EM monitoring—acquisition and inversion. In: 72nd EAGE conference, Barcelona, Spain, extended abstract
- Routh PS, Oldenburg DW (1999) Inversion of controlled source audiofrequency magnetotellurics data for a horizontally layered earth. *Geophysics* 64(6):1689–1697
- Rust WM Jr (1938) A historical review of electrical prospecting methods. *Geophysics* 3(1):1–6
- San Filipo WA, Hohmann GW (1983) Computer simulation of low-frequency electromagnetic data acquisition. *Geophysics* 48(9):1219–1232
- Sandberg SK, Hohmann GW (1982) Controlled-source audiomagnetotellurics in geothermal exploration. *Geophysics* 47(1):100–116

- Schaller A, Hunziker J, Streich R, Drijkoningen G (2014) Sensitivity of the near-surface vertical electric field in land controlled-source electromagnetic monitoring. In: 84th SEG annual meeting, Denver, extended abstract
- Schamper C, Rejiba F, Tabbagh A, Spitz S (2011) Theoretical analysis of long offset time-lapse frequency domain controlled source electromagnetic signals using the method of moments: application to the monitoring of a land oil reservoir. *J Geophys Res-Solid Earth* 116(B3):B03101
- Schlumberger C (1920) Study of underground electrical prospecting. Paris, translated to English by Kelly SF
- Schön JH (2004) Physical properties of rocks: fundamentals and principles of petrophysics. Elsevier, Amsterdam
- Schwarzbach C, Börner R-U, Spitzer K (2011) Three-dimensional adaptive higher order finite element simulation for geo-electromagnetics—a marine CSEM example. *Geophys J Int* 187:63–74
- Schwarzbach C, Haber E (2013) Finite element based inversion for time-harmonic electromagnetic problems. *Geophys J Int* 193(2):615–634
- Sheard S, Ritchie T, Christopherson KR, Brand E (2005) Mining, environmental, petroleum, and engineering industry applications of electromagnetic techniques in geophysics. *Surv Geophys* 26(5):653–669
- Siemon B, Christiansen AV, Auken E (2009) A review of helicopter-borne electromagnetic methods for groundwater exploration. *Near Surf Geophys* 7(5–6):629–646
- Smith R (2014) Electromagnetic induction methods in mining geophysics from 2008 to 2012. *Surv Geophys* 35:123–156
- Spies BR (1983) Recent developments in the use of surface electrical methods for oil and gas exploration in the Soviet Union. *Geophysics* 48(8):1102–1112
- Spies BR (1988) Local noise prediction filtering for central induction transient electromagnetic sounding. *Geophysics* 53(8):1068–1079
- Spies BR, Eggers DE (1986) The use and misuse of apparent resistivity in electromagnetic methods. *Geophysics* 51(7):1462–1471
- Spies B R, Frischknecht FC (1991) Electromagnetic sounding. In: Nabighian MN (ed) *Electromagnetic methods in applied geophysics*, vol 2. Society of Exploration Geophysicists, pp 285–425
- Smrka LJ, Carozzone JJ, Ephron MS, Eriksen EA (2006) Remote reservoir resistivity mapping. *Lead Edge* 25(8):972–975
- Statham L (1936) Electric earth transients in geophysical prospecting. *Geophysics* 1(2):271–277
- Statham L (1939) Method and apparatus for comparing electrical transients. United States Patent 2,113,749
- Stephan A, Strack K-M (1991) A simple approach to improve the S/N ratio for TEM data using multiple receivers. *Geophysics* 56(6):863–869
- Sternberg BK, Washburne JC, Pellerin L (1988) Correction for the static shift in magnetotellurics using transient electromagnetic soundings. *Geophysics* 53(11):1459–1468
- Sternberg BK (1979) Electrical resistivity structure of the crust in the southern extension of the Canadian Shield Layered Earth models. *J Geophys Res-Solid Earth* 84(B1):212–228
- Strack K (2014) Future directions of electromagnetic methods for hydrocarbon applications. *Surv Geophys* 35(1):157–177
- Strack KM (1992) *Exploration with deep transient electromagnetics*. Elsevier, Amsterdam
- Strack KM (2004) Combined surface and wellbore electromagnetic measurement system and method for determining formation fluid properties. United States Patent 6,739,165 B1
- Strack K-M, Hanstein T, Lelsroq K, Moss DC, Vozoff K, Wolfgram PA (1989a) Case histories of LOTEM surveys in hydrocarbon prospective areas. *First Break* 7(12):467–477
- Strack K-M, Hanstein TH, Eilenz HN (1989b) LOTEM data processing for areas with high cultural noise levels. *Phys Earth Planet Inter* 53:261–269
- Stratton JA (1941) *Electromagnetic theory*. McGraw-Hill, New York
- Streich R (2009) 3D finite-difference frequency-domain modeling of controlled-source electromagnetic data: direct solution and optimization for high accuracy. *Geophysics* 74(5):F95–F105
- Streich R, Becken M (2011) Electromagnetic fields generated by finite-length wire sources: comparison with point dipole solutions. *Geophys Prospect* 59:361–374
- Streich R, Becken M, Matzander U, Ritter O (2011) Strategies for land-based controlled-source electromagnetic surveying in high-noise regions. *Lead Edge* 30(10):1174–1181
- Streich R, Becken M, Ritter O (2010) Imaging of CO₂ storage sites, geothermal reservoirs, and gas shales using controlled-source magnetotellurics: Modeling studies. *Chemie der Erde (Geochemistry)* 70(S3):63–75
- Streich R, Becken M, Ritter O (2013) Robust processing of noisy land-based controlled-source electromagnetic data. *Geophysics* 78(5):E237–E247

- Sudha A, Tezkan B, Siemon B (2014) Appraisal of a new 1D weighted joint inversion of ground based and helicopter-borne electromagnetic data. *Geophys Prospect* 62(3):597–614
- Sundberg K (1930) Electrical prospecting for oil structure. *AAPG Bull* 14(9):1145–1163
- Swidinsky A, Edwards RN, Jegen M (2013) The marine controlled source electromagnetic response of a steel borehole casing: applications for the NEPTUNE Canada gas hydrate observatory. *Geophys Prospect* 61(4):842–856
- Szarka L (1988) Geophysical aspects of man-made electromagnetic noise in the earth. *Surv Geophys* 9:287–318
- Szarka L (2009) Early analogue modeling experiments and related studies to today's problems of geoelectromagnetic exploration. *J Earth Sci* 20:618–625
- Tanbo T, Sakai H, Nagao T (2003) A study of geoelectric potential change caused by rail leak current observed at Ohtawa, Gifu, Japan. *Electr Eng Jpn* 143(2):1–10 (Translated from *Denki Gakkai Ronbunshi*, Vol. 122-A, No. 5, May 2002, pp. 446453)
- Tang JT, He JS (2000) Controlled source audio magnetotelluric method and its application, Chinese edn. China Press
- Tietze K, Ritter O (2014) Electromagnetic monitoring of the propagation of an injected polymer for enhanced oil recovery in Northern Germany. In: 76th EAGE conference and exhibition, Amsterdam, extended abstract
- Tietze K, Ritter O, Veeken P (2015) Controlled-source electromagnetic monitoring of reservoir oil-saturation using a novel borehole-to-surface configuration. *Geophys Prospect* (in press)
- Tikhonov AN, Arsenin VY (1977) Solutions of ill-posed problems. Winston VH and Sons, Washington
- Tøndel R, Schütt H, Dümmonig S, Ducrocq A, Godfrey R, LaBrecque D, Nutt L, Campbell A, Rufino R (2014) Reservoir monitoring of steam-assisted gravity drainage using borehole measurements. *Geophys Prospect* 62(4):760–778
- Torres-Verdín C, Habashy TM (1994) Rapid 2.5-dimensional forward modeling and inversion via a new nonlinear scattering approximation. *Radio Sci* 29(4):1051–1079
- Tseng H-W, Becker A, Wilt MJ, Deszcz-Pan M (1998) A borehole-to-surface electromagnetic survey. *Geophysics* 63(5):1565–1572
- Ucok H, Ershaghi I, Olhoeft GR (1980) Electrical resistivity of geothermal brines. *J Petrol Technol* 32(4):717–727
- Um ES, Commer M, Newman GA (2014) A strategy for coupled 3D imaging of large-scale seismic and electromagnetic data sets: application to subsalt imaging. *Geophysics* 79(3):ID1–ID13
- Um ES, Alumbaugh DL (2007) On the physics of the marine controlled-source electromagnetic method. *Geophysics* 72(2):WA13–WA26
- Um ES, Commer M, Newman GA (2013) Efficient pre-conditioned iterative solution strategies for the electromagnetic diffusion in the Earth: finite-element frequency-domain approach. *Geophys J Int* 193:1460–1473
- Unsworth M, Oldenburg D (1995) Subspace inversion of electromagnetic data: application to mid-ocean-ridge exploration. *Geophys J Int* 123(1):161–168
- van Zijl JSV, Joubert SJ (1975) A crustal geoelectrical model for South African Precambrian granitic terrains based on deep Schlumberger soundings. *Geophysics* 40(4):657–663
- Vanyan LL, Bobrovnikov LZ, Loshenitzina VL, Davidov VM, Morozova GM, Kuznetsov AN, Shtimmer AI, Terekhin EI (1967) Electromagnetic depth soundings. Consultants Bureau, New York (translated from Russian by Keller GV)
- Velikhov EP, Grigoriev VF, Zhdanov MS, Korotayev SM, Kruglyakov MS, Orekhova DA, Popova IV, Tereschenko ED, Schors YG (2011) Electromagnetic sounding of the Kola Peninsula with a powerful extremely low frequency source. *Dokl Earth Sci* 438(1):711–716
- Velikhov YP, Zhdanov MS, Frenkel MA (1987) Interpretation of MHD-sounding data from the Kola Peninsula by the electromagnetic migration method. *Phys Earth Planet Inter* 45(2):149–160
- Vilamajó E, Queralt P, Ledo J, Marcuello A (2013) Feasibility of monitoring the Hontomín (Burgos, Spain) CO₂ storage site using a deep EM source. *Surv Geophys* 34(4):441–461
- Vilamajó E, Rondeleux B, Bourgeois B, Queralt P, Marcuello A, Ledo J (2014) First results of the baseline EM monitoring experiments at the hontomín CO₂ storage site (Spain): LEMAM and borehole-to-surface CSEM. In: IAGA WG 1.2 workshop on electromagnetic induction in the earth, Weimar, Germany
- Vozoff K, Jupp DLB (1975) Joint inversion of geophysical data. *Geophys J R Astr S* 42:977–991
- Wait JR (1951a) A conducting sphere in a time varying magnetic field. *Geophysics* 16(4):666–672
- Wait JR (1951b) Transient electromagnetic propagation in a conducting medium. *Geophysics* 16(2):213–221

- Wait JR (1952) The cylindrical ore body in the presence of a cable carrying an oscillating current. *Geophysics* 17(2):378–386
- Wait JR (1954) On the relation between telluric currents and the Earth's magnetic field. *Geophysics* 19(2):281–289
- Wait JR (1962) Electromagnetic waves in stratified media. International series of monographs on electromagnetic waves. Pergamon Press, New York
- Wait JR (1972) The effect of a buried conductor on the subsurface fields for line source excitation. *Radio Sci* 7(5):587–591
- Wait JR (1982) *Geo-electromagnetism*. Academic Press, New York
- Wait JR (1983) Mutual coupling between grounded circuits and the effect of a thin vertical conductor in the earth. *IEEE Trans Antenna Propag* 31(4):640–644
- Wait JR, Williams JT (1985) EM and IP response of a steel well casing for a four-electrode surface array. Part I: theory. *Geophys Prospect* 33:723–735
- Wang T, Oristaglio M, Tripp A, Hohmann G (1994) Inversion of diffusive transient electromagnetic data by a conjugate-gradient method. *Radio Sci* 29(4):1143–1156
- Wannamaker PE (1997) Tensor CSAMT survey over the Sulphur Springs thermal area, Valles Caldera, New Mexico, U.S.A., Part II: implications for CSAMT methodology. *Geophysics* 62(2):466–476
- Wannamaker PE (2005) Anisotropy versus heterogeneity in continental solid earth electromagnetic studies: fundamental response characteristics and implications for physiochemical state. *Surv Geophys* 26:733–765
- Ward SH (1980) History of geophysical exploration: electrical, electromagnetic, and magnetotelluric methods. *Geophysics* 45(11):1659–1666
- Weidelt P (2007a) Guided waves in marine CSEM. *Geophys J Int* 171:153–176
- Weidelt P (2007b) Guided waves in marine CSEM and the adjustment distance in MT: a synopsis. In: *Protokoll über das Kolloquium Elektromagnetische Tiefenforschung*, pp 1–17
- Weiss CJ, Constable S (2006) Mapping thin resistors and hydrocarbons with marine EM methods, part II—modeling and analysis in 3D. *Geophysics* 71(6):G321–G332
- West GF, Macnae JC, Lamontagne Y (1984) A time-domain EM system measuring the step response of the ground. *Geophysics* 49(7):1010–1026
- Wilson AJS (1997) The equivalent wavefield concept in multichannel transient electromagnetic surveying. Ph.D. thesis, University of Edinburgh
- Wilt M, Goldstein NE, Stark M, Haught JR, Morrison HF (1983) Experience with the EM-60 electromagnetic system for geothermal exploration in Nevada. *Geophysics* 48(8):1090–1101
- Wilt MJ, Morrison HF, Lee KH, Goldstein NE (1989) Electromagnetic sounding in the Columbia Basin, Yakima, Washington. *Geophysics* 54(8):952–961
- Wirianto M, Mulder WA, Slob EC (2010) A feasibility study of land CSEM reservoir monitoring in a complex 3-D model. *Geophys J Int* 181:741–755
- Wirianto M, Mulder WA, Slob EC (2011) Exploiting the airwave for time-lapse reservoir monitoring with CSEM on land. *Geophysics* 76(3):A15–A19
- Won IJ (1980) A wideband electromagnetic exploration method—some theoretical and experimental results. *Geophysics* 45(5):928–940
- Wright D, Ziolkowski A, Hobbs B (2002) Hydrocarbon detection and monitoring with a multicomponent transient electromagnetic (MTEM) survey. *Lead Edge* 21(9):852–864
- Wright DA, Ziolkowski AM, Hobbs BA (2005) Detection of subsurface resistivity contrasts with application to location of fluids. US Patent 6,914,433 B2
- Wu X, Habashy TM (1994) Influence of steel casings on electromagnetic signals. *Geophysics* 59(3):378–390
- Yost WJ (1952) The interpretation of electromagnetic reflection data in geophysical exploration—part I, general theory. *Geophysics* 17(1):89–106
- Zhamaletdinov AA, Shevtsov AN, Korotkova TG, Kopytenko YA, Ismagilov VS, Petrishev MS, Efimov BV, Barannik MB, Kolobov VV, Prokopchuk PI, Smirnov MY, Vagin SA, Pertel MI, Tereshchenko ED, Vasilev AN, Grigoryev VF, Gokhberg MB, Trofimchik VI, Yampolsky YM, Koloskov AV, Fedorov AV, Korja T (2011) Deep electromagnetic sounding of the lithosphere in the Eastern Baltic (Fennoscandian) Shield with high-power controlled sources and industrial power transmission lines (FENICS experiment). *Izvestiya Phys Solid Earth* 47(1):2–22
- Zhdanov M (2009) Geophysical electromagnetic theory and methods. In: *Methods in geochemistry and geophysics*, vol 43. Elsevier, Amsterdam
- Zhdanov MS (2010) Electromagnetic geophysics: notes from the past and the road ahead. *Geophysics* 75(5):75A49–75A66
- Zhdanov MS (2012) Reply to the discussion. *Geophysics* 75(2):X10–X11

- Zhdanov MS, Endo M, Black N, Spangler L, Fairweather S, Hibbs A, Eiskamp GA, Will R (2013) Electromagnetic monitoring of CO₂ sequestration in deep reservoirs. *First Break* 31(2):71–78
- Zhdanov MS, Keller GV (1994) The geoelectrical methods in geophysical exploration. In: *Methods in geochemistry and geophysics*, vol 31. Elsevier, Amsterdam
- Ziolkowski A, Hobbs B, Wright D (2002) First direct hydrocarbon detection and reservoir monitoring using transient electromagnetics. *First Break* 20(4):224–225
- Ziolkowski A, Hobbs BA, Wright D (2007) Multitransient electromagnetic demonstration survey in France. *Geophysics* 72(4):F197–F209
- Ziolkowski A, Parr R, Wright D, Nockles V, Limond C, Morris E, Linfoot J (2010) Multi-transient electromagnetic repeatability experiment over the North Sea Harding field. *Geophys Prospect* 58:1159–1176
- Zonge KL, Hughes LJ (1991) Controlled-source audio-frequency magnetotellurics. In: Nabighian MN (ed) *Electromagnetic methods in applied geophysics*. Society of Exploration Geophysicists, Tulsa, pp 713–809